

Expanding a fluorescent RNA Alphabet: synthesis, photophysics and utility of isothiazole-derived purine nucleoside surrogates

Alexander R. Rovira, Andrea Fin, and Yitzhak Tor*

Supplementary Information

| | |
|--|------------|
| 1. Materials and methods | S2 |
| 1.1. Abbreviations | S2 |
| 2. Synthetic procedures | S2 |
| 3. Structural analysis | S13 |
| 3.1. Experimental summary | S13 |
| 3.2. X-ray crystal structures | S14 |
| 3.3. Crystal structure overlay | S17 |
| 4. Absorption and emission spectroscopy | S18 |
| 4.1. General | S18 |
| 4.2. Fluorescence quantum yield evaluation | S19 |
| 4.3. Sensitivity to pH | S19 |
| 4.4. Sensitivity to polarity | S24 |
| 5. Enzymatic conversion by adenosine deaminase | S25 |
| 5.1. General methods | S25 |
| 5.2. Steady state absorption and emission experiments with adenosine deaminase | S25 |
| 5.3. Fluorescence based kinetic assays in presence of ADA | S27 |
| 5.4. HPLC analysis for the adenosine deaminase mediated conversion | S27 |
| 5.4.1. General | S27 |
| 5.4.2. LC analysis for the enzymatic conversion of ¹² 2-AA to ¹² G | S27 |
| 5.5. HPLC analysis for the competitive enzymatic deamination | S30 |
| 6. Supplementary figures | S37 |
| 6.1. ¹ H- and ¹³ C-NMR spectra | S36 |
| 7. Supplementary references | S52 |

1. Materials and Methods

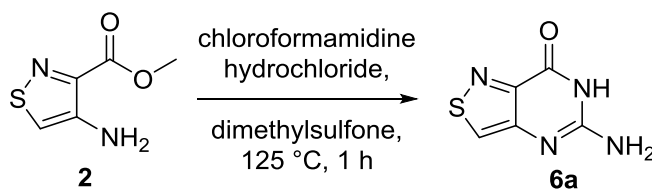
Reagents were purchased from Sigma-Aldrich, Fluka, TCI, and Acros and were used without further purification unless otherwise specified. Solvents were purchased from Sigma-Aldrich and Fisher Scientific, and dried by standard techniques. NMR solvents were purchased from Cambridge Isotope Laboratories (Andover, MA). All reactions were monitored with analytical TLC (Merck Kieselgel 60 F254). Column chromatography was carried out with Teledyne ISCO Combiflash Rf with silica gel particle size 40-63 μm . NMR spectra were obtained on Varian Mercury 400 MHz and Varian VX 500 MHz. Mass spectra were obtained on an Agilent 6230 HR-ESI-TOF MS at the Molecular Mass Spectrometry Facility at the UCSD Chemistry and Biochemistry Department.

1.1. Abbreviations

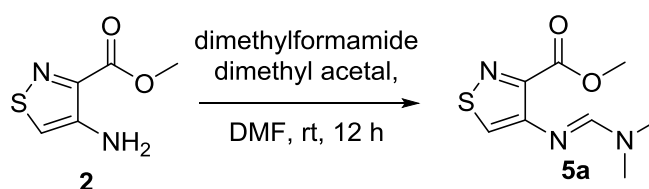
ACN: acetonitrile; DCM: dichloromethane; DMF: *N,N*-dimethylformamide; DMSO: dimethyl sulfoxide; Et₂O: diethyl ether; EtOAc: ethyl acetate; EtOH: ethanol; MeOH: methanol; NaOMe: sodium methoxide; rt: room temperature; TEA: triethylamine; POCl₃: phosphorus(V) oxychloride; EDCI: 1-Ethyl-3-(3-dimethylaminopropyl)carbodiimide.

2. Synthetic procedures

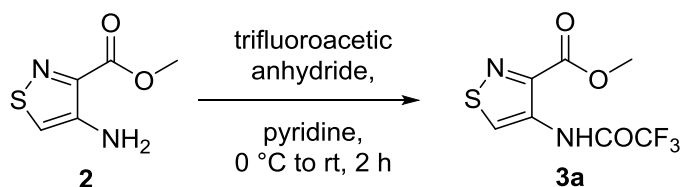
Methyl 4-aminoisothiazole-3-carboxylate HCl salt (2), compounds **13-20**, **24**, **25**, ^{tz}**G**, ^{tz}**A**, and ^{tz}**I** were prepared according to previously reported procedures.^{S1} Chloroformamidine hydrochloride was prepared according to a previously reported procedure.^{S2} 1,4-Anhydro-3-O-(tert-butylidiphenylsilyl)-2-deoxy-Derythro-pent-1-enitol (**9**) was synthesized according to a previously reported procedure.^{S3} 1-O-Acetyl-tri-benzoyl- β -D-ribofuranose and 2,3:5,6-Di-O-isopropylidene- α -D-mannofuranose (**10**) were purchased from Sigma Aldrich. 3,5-O-((1,1,3,3-tetraisopropyl)disiloxanediyl)-2-deoxy-D-ribo-1,4-lactone (**11**) was synthesized according to a previously reported procedure.^{S4}



5-aminoisothiazolo[4,3-d]pyrimidin-7(6H)-one (2). A well-mixed fine solid of **2** (1.00 g, 5.14 mmol) and chloroformamidinium hydrochloride (0.59 g, 5.14 mmol) was added to dimethylsulfone (14.51 g) at 125 °C over 10 minutes, and the resulting solution was stirred for 1 hour at the same temperature. Upon cooling to room temperature, the mixture was poured into water (50 mL), basified with concentrated NH₄OH and vigorously stirred for 1 hour. The resulting creamy solid was filtered, washed with water (50 mL), Et₂O (20 mL), and dried under vacuum. The resulting solid (0.64 g, 74 %) was used for the next step without further purification. ¹H NMR (500 MHz, DMSO): δ 11.05 (br s, 1H), 8.62 (s, 1H), 6.34 (br s, 2H); ¹³C NMR (125 MHz, DMSO): δ 156.97, 151.90, 150.50, 149.06; ESI-HRMS calcd for [C₅H₃N₄OS]⁻ [M-H]⁻ 167.0033, found 167.0032.

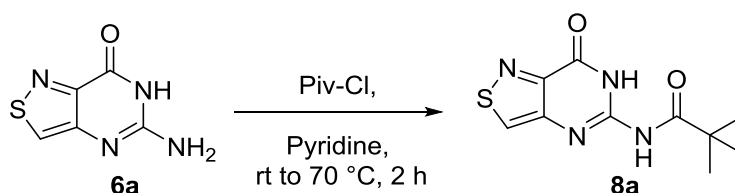


Methyl (E)-4-(((dimethylamino)methylene)amino)isothiazole-3-carboxylate (5a). In a 10 mL round bottom flask with stir bar, **2** (0.12 g, 0.73 mmol) was dissolved in anhydrous DMF (3.64 mL) stirring at room temperature under argon followed by addition of N,N-dimethylformamide dimethyl acetal (0.58 mL, 4.36 mmol). The reaction was left to stir at room temperature for 12 hours. The reaction was then partitioned between EtOAc and water. The aqueous layer was washed several times with EtOAc and the organic solution was washed once with brine before being dried over Na₂SO₄ and evaporated to dryness. The resulting residue was purified by column chromatography (0% MeOH to 5% MeOH in DCM) yielding a white solid (57 mg, 37%). R_f 0.58 in 10% MeOH in DCM. ¹H NMR (500 MHz, CDCl₃): δ 7.95 (s, 1H), 7.61 (s, 1H), 3.90 (s, 3H), 3.03 (s, 6H); ¹³C NMR (125 MHz, CDCl₃): δ 161.66, 155.21, 151.48, 151.26, 133.19, 52.39, 40.41, 34.51. ESI-HRMS calcd for [C₈H₁₂N₃O₂S]⁺ [M+H]⁺ 214.0645, found 214.0640.

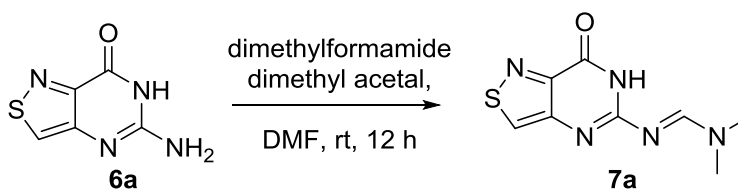


Methyl 4-(2,2,2-trifluoroacetamido)isothiazole-3-carboxylate (3a). In a 50 mL round bottom flask, **2** (1.00 g, 5.14 mmol) was dissolved in anhydrous pyridine (20 mL) stirring at 0 °C in an ice bath followed by dropwise addition of trifluoroacetic anhydride (1.45 mL, 10.28 mmol) and left to stir under argon for 2 hours, slowly warming to room temperature. After the reaction was complete, as monitored by TLC, the organic

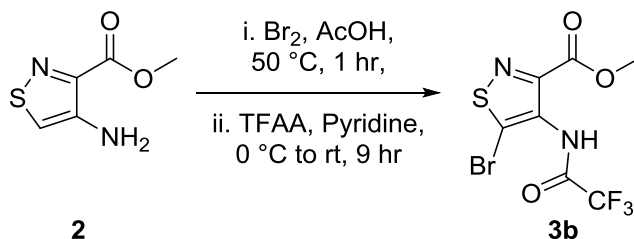
solution was evaporated to dryness and the resulting residue was subjected to purification by column chromatography (0% EtOAc to 30% EtOAc in Hexanes) yielding white translucent crystals (1.10 g, 84%). R_f 0.58 in 40% EtOAc in hexanes. $^1\text{H NMR}$ (500MHz, CDCl_3): δ 10.96 (br s, 1H), 9.42 (s, 1H), 4.06 (s, 3H); $^{13}\text{C NMR}$ (125MHz, CDCl_3): δ 163.00, 154.70 (q), 145.81, 137.40, 134.20, 115.50 (q), 53.45; ESI-HRMS calcd for $[\text{C}_7\text{H}_4\text{F}_3\text{N}_2\text{O}_3\text{S}]^-$ $[\text{M}-\text{H}]^-$ 252.9900, found 252.9902.



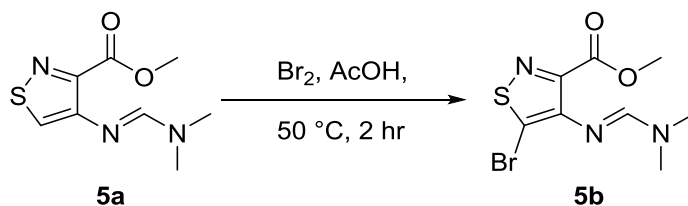
N-(7-oxo-6,7-dihydroisothiazolo[4,3-d]pyrimidin-5-yl)pivalamide (8a). In a flame-dried 10 mL round bottom flask with stir bar, **6a** (85 mg, 0.51 mmol) was dissolved in anhydrous pyridine (2 mL) stirring at room temperature under argon followed by dropwise addition of pivaloyl chloride (75 μL , 0.61 mmol) and left to stir at 70 $^\circ\text{C}$ for 2 hours. The solution was then cooled to room temperature and evaporated to dryness. The resulting residue was subjected to purification by column chromatography (0% EtOAc to 50% EtOAc in Hexanes) yielding a white powder (60 mg, 47%). R_f 0.12 in 40% EtOAc in hexanes. $^1\text{H NMR}$ (500 MHz, CDCl_3): δ 8.65 (s, 1H), 1.33 (s, 9H); $^{13}\text{C NMR}$ (125 MHz, CDCl_3): δ 180.30, 154.86, 149.13, 147.35, 146.40, 140.67, 40.36, 26.99; ESI-HRMS calcd for $[\text{C}_{10}\text{H}_{11}\text{N}_4\text{O}_2\text{S}]^-$ $[\text{M}-\text{H}]^-$ 251.0608, found 251.0607.



(E)-N,N-dimethyl-N'-(7-oxo-6,7-dihydroisothiazolo[4,3-d]pyrimidin-5-yl)formimidamide (7a). In a flame dried 10mL flask with stir bar, **6a** (0.10 g, 0.59 mmol) was dissolved in DMF (6 mL) stirring at room temperature followed by addition of N,N-dimethylformamide dimethyl acetal (0.64 mL, 4.76 mmol) and left to stir for 12 hours. After the reaction was completed as monitored by TLC, the solution was partitioned between EtOAc and water. After several aqueous washes, the organic solution was dried over Na_2SO_4 and evaporated to dryness to yield a crude oil. The compound was purified by column chromatography (0% MeOH to 5% MeOH in DCM) to yield a yellow solid (0.12 g, 90%). R_f 0.54 in 10% MeOH in DCM. $^1\text{H NMR}$ (500 MHz, CDCl_3): δ 8.70 (s, 1H), 8.59 (s, 1H), 3.21 (s, 3H), 3.13 (s, 3H); $^{13}\text{C NMR}$ (125 MHz, CDCl_3): δ 158.08, 156.67, 154.87, 151.86, 149.48, 138.31, 41.48, 35.27; ESI-HRMS calcd for $[\text{C}_8\text{H}_9\text{N}_5\text{OSNa}]^+$ $[\text{M}+\text{H}]^+$ 246.0420, found 246.0418.

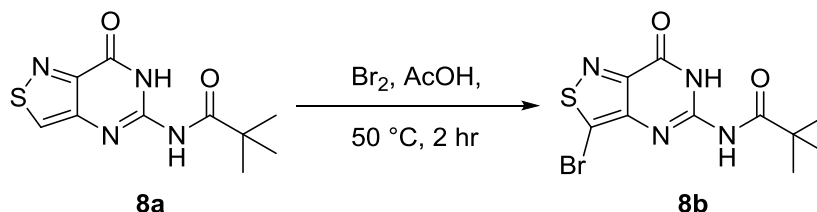


Methyl 5-bromo-4-(2,2,2-trifluoroacetamido)-isothiazole-3-carboxylate (3b). In an 8 mL reaction vial with stir bar, **2** (35 mg, 0.22 mmol) was dissolved in acetic acid (2.2 mL) at room temperature followed by bromine (0.02 mL, 0.44 mmol) and the vial was sealed. The reaction was left to stir at 55 °C monitoring by TLC. After 1 hour stirring, starting material was found to be consumed. The vial was cooled to 0 °C and all solvent was removed under pressure. The vial was then treated with pyridine (2 mL) and brought to 0 °C stirring for 5 minutes before addition of trifluoroacetic anhydride (0.05 mL, 0.33 mmol) and left to warm up to room temperature. After 9 hours stirring, starting material is found to be consumed. The solvent was removed under pressure and the resulting residue was partitioned between water and ethyl acetate. The aqueous layer was extracted with ethyl acetate three times before the organic solution was washed with saturated sodium thiosulfate and brine solutions followed by saturated sodium sulfate. The organic solution was evaporated to dryness to yield a crude oil. The compound was purified by column chromatography (0% EtOAc to 40% EtOAc in Hexanes) to yield a yellow solid (34 mg, 65%). R_f 0.46 in 40% EtOAc in hexanes. $^1\text{H NMR}$ (500 MHz, CDCl_3): δ 9.05 (br s, 1H), 4.01 (s, 3H); $^{13}\text{C NMR}$ (125 MHz, CDCl_3): δ 160.82, 154.25 (q), 150.84, 132.87, 132.67, 116.70 (q), 53.40. ESI-HRMS calcd for $[\text{C}_7\text{H}_3\text{BrF}_3\text{N}_2\text{O}_3\text{S}]^-$ $[\text{M}-\text{H}]^-$ 330.9005, found 330.9006.

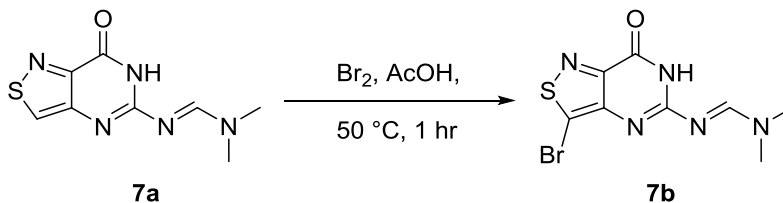


Methyl (E)-5-bromo-4-(((dimethylamino)methylene)amino)isothiazole-3-carboxylate (5b). In a flame-dried 8 mL reaction vial with stir bar, protected ester **5a** (13 mg, 0.06 mmol) was dissolved in acetic acid (1.2 mL) followed by dropwise bromine (0.01 mL, 0.19 mmol) and left to stir at 50 °C for 2 hours until the reaction was found to be complete as monitored by TLC. The reaction was then partitioned between EtOAc and water followed by neutralization of the aqueous solution with NaHCO_3 . After the aqueous solution was washed several times with EtOAc, the organic solution was washed with brine and dried over Na_2SO_4 . After evaporation to dryness, the resulting residue was purified by column chromatography (0%

MeOH to 3% MeOH in DCM) to yield a yellow solid (7 mg, 39%). R_f 0.74 in 10% MeOH in DCM. $^1\text{H NMR}$ (500 MHz, CDCl_3): δ 7.52 (s, 1H), 3.90 (s, 3H), 3.10 (s, 3H), 3.06 (s, 6H); $^{13}\text{C NMR}$ (125 MHz, CDCl_3): δ 160.95, 156.06, 151.29, 148.87, 124.17, 52.58, 40.55, 34.55. ESI-HRMS calcd for $[\text{C}_8\text{H}_{11}\text{BrN}_3\text{O}_2\text{S}]^+$ $[\text{M}+\text{H}]^+$ 291.9750, found 291.9751.

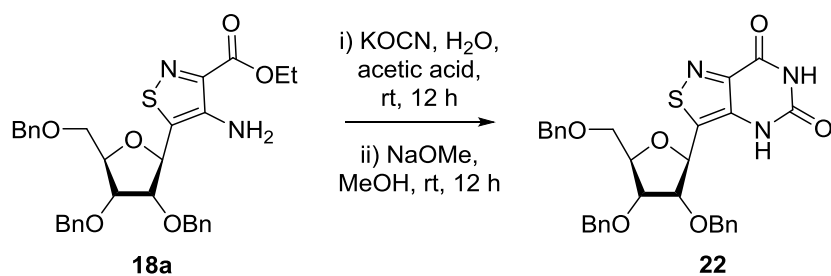


N-(3-bromo-7-oxo-6,7-dihydroisothiazolo[4,3-d]pyrimidin-5-yl)pivalamide (8b). To a flame-dried 8mL reaction vial with stir bar, pivaloyl-protected nucleobase **8a** (0.02 g, 0.08 mmol) was dissolved in acetic acid (1.56 mL) followed by dropwise bromine (12 μL , 0.24 mmol) and left to stir at 50 °C for 2 hours until the reaction was found to be complete as monitored by TLC. The reaction was then partitioned between EtOAc and water followed by neutralization of the aqueous solution with NaHCO_3 . After the aqueous solution was washed several times with EtOAc, the organic solution was washed with brine and dried over Na_2SO_4 . After evaporation to dryness, the resulting residue was purified by column chromatography (0% EtOAc to 40% EtOAc in Hexanes) to yield a yellow solid (12 mg, 46%). R_f 0.42 in 40% EtOAc in Hexanes. $^1\text{H NMR}$ (500 MHz, CDCl_3): δ 12.27 (br s, 1H), 8.75 (br s, 1H), 1.35 (s, 9H); $^{13}\text{C NMR}$ (125 MHz, CDCl_3): δ 180.40, 154.38, 148.83, 147.17, 145.97, 128.98, 40.47, 27.00; ESI-HRMS calcd for $[\text{C}_{10}\text{H}_{10}\text{BrN}_4\text{O}_2\text{S}]^-$ $[\text{M}-\text{H}]^-$ 328.9713 found 328.9710.

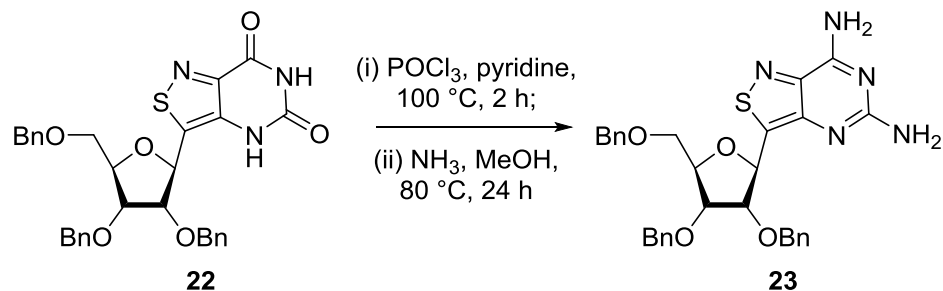


(E)-N'-(3-bromo-7-oxo-6,7-dihydroisothiazolo[4,3-d]pyrimidin-5-yl)-N,N-dimethylformimidamide (7b). In a flame-dried 8mL reaction vial with stir bar, protected nucleobase **7a** (75 mg, 0.34 mmol) is dissolved in acetic acid (3.4 mL) followed by dropwise bromine (52 μL , 1.00 mmol) and left to stir at 50 °C for 1 hour until the reaction was found to be complete as monitored by TLC. The reaction was then partitioned between EtOAc and water followed by neutralization of the aqueous solution with NaHCO_3 . After the aqueous solution was washed several times with EtOAc, the organic solution was washed with brine

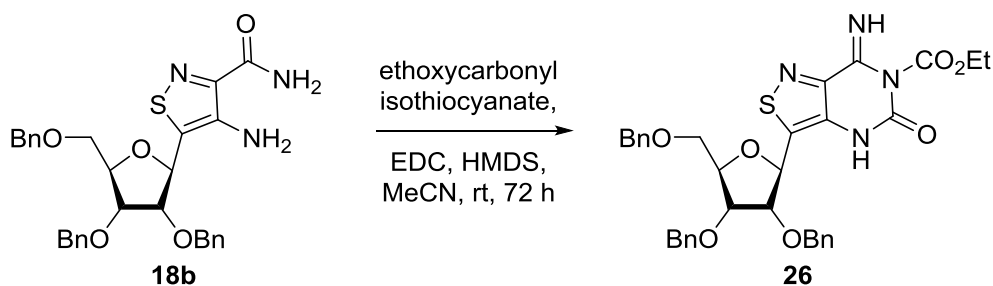
and dried over Na₂SO₄. After evaporation to dryness, the resulting residue was purified by column chromatography (0% MeOH to 5% MeOH in DCM) to yield a yellow powder (55 mg, 54%). R_f 0.48 in 10% MeOH in 90% DCM. ¹H NMR (500 MHz, CDCl₃): δ 8.75 (s, 1H), 3.24 (s, 3H), 3.14 (s, 3H); ¹³C NMR (125 MHz, CDCl₃): δ 158.34, 156.47, 155.37, 151.86, 149.43, 147.86, 41.64, 35.42; ESI-HRMS calcd for [C₈H₇BrN₅OS]⁻ [M-H]⁻ 299.9560, found 299.9560.



3-((2R,3S,4S,5R)-3,4-bis(benzyloxy)-5-((benzyloxy)methyl)tetrahydrofuran-2-yl)isothiazolo[4,3-d]pyrimidine-5,7(4H,6H)-dione (22). In a 10 mL round bottom flask with stir bar, **18a** (130 mg, 0.23 mmol) was dissolved acetic acid (2.26 mL) stirring at room temperature. Potassium cyanate (55 mg, 0.68 mmol) was added and the reaction was left to stir under argon over 12 hours. The reaction was then partitioned between EtOAc and water. The aqueous solution was neutralized and washed several times with EtOAc. The organic solution was washed with brine, dried over Na₂SO₄, and evaporated to dryness. The resulting residue (0.11 g, 0.18 mmol) was flushed with argon and used crude. Anhydrous MeOH (1.78 mL) was added followed by mild heating to dissolve the substrate. After cooling to room temperature, the solution was treated with sodium methoxide (5 M, 1.07 mL, 0.53 mmol) and left to stir under argon at room temperature for 12 hours. The reaction was then quenched with water and diluted with EtOAc. The aqueous solution was washed several times with EtOAc and the organic solution was washed with brine and dried over Na₂SO₄. The resulting organic solution was then evaporated to dryness and subjected to purification by column chromatography (Hexanes/EtOAc with a gradient from 0% to 70% of EtOAc) to yield a white foam (75 mg, 74%). R_f 0.13 in 60/40 Hexanes/EtOAc. ¹H NMR (500 MHz, CDCl₃): δ 9.61 (s, 1H), 8.06 (s, 1H), 7.40–7.08 (m, 15H), 5.22 (d, *J* = 8.2 Hz, 1H), 4.97 (d, *J* = 12.5 Hz, 1H), 4.62 (dd, *J* = 11.9, 2.1 Hz, 2H), 4.52 (m, 2H), 4.33 (d, *J* = 11.9 Hz, 1H), 4.29 (d, *J* = 1.5 Hz, 1H), 4.02 (dd, *J* = 8.2, 4.9 Hz, 1H), 3.92 (dd, *J* = 4.9, 2.2 Hz, 1H), 3.73 (dd, *J* = 10.5, 2.8 Hz, 1H), 3.45 (dd, *J* = 10.5, 1.2 Hz, 1H); ¹³C NMR (125 MHz, CDCl₃): δ 155.60, 149.15, 146.05, 144.86, 137.14, 136.71, 136.25, 134.91, 128.66, 128.59, 128.43, 128.40, 128.36, 128.35, 128.18, 128.10, 83.41, 81.06, 75.85, 73.16, 72.96, 72.50, 68.75; ESI-HRMS calcd for [C₃₁H₂₈N₃O₆S]⁻ [M-H]⁻ 570.1704, found 570.1699.

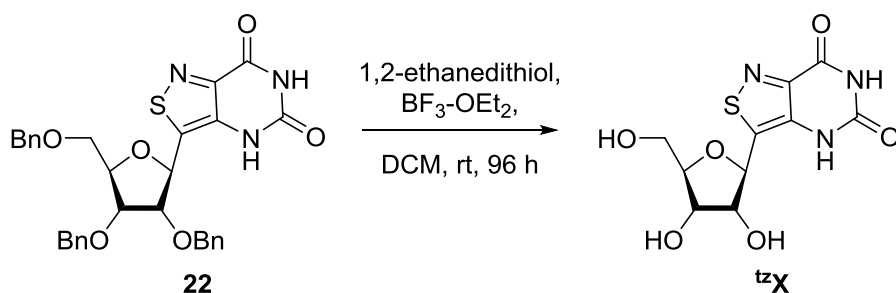


3-((2R,3S,4S,5R)-3,4-bis(benzyloxy)-5-((benzyloxy)methyl)tetrahydrofuran-2-yl)isothiazolo[4,3-d]pyrimidine-5,7-diamine (23). To an 8 mL reaction vial with stir bar containing the protected nucleoside **22** (0.17 g, 0.30 mmol), pyridine (48 μ L, 0.59 mmol) was added followed by POCl₃ (2.77 mL, 29.7 mmol) and left to stir under reflux conditions at 115 °C for 2 hours before removing the reaction vial from heat and evaporating to dryness. The resulting oil was dissolved in cold methanol that has been saturated with ammonia at 0 °C. The vial was capped and left to stir at 80 °C for 24 hours. The reaction was then evaporated to dryness and subjected to purification by column chromatography (Hexanes/EtOAc with a gradient from 0% to 80% of EtOAc) to yield a white foam (0.04 g, 24%). R_f 0.15 in 60/40 Hexanes/EtOAc. ¹H NMR (500 MHz, CD₃OD): δ 7.36–7.08 (m, 15H), 5.58 (d, *J* = 5.3 Hz, 1H), 4.64–4.48 (m, 5H), 4.47–4.42 (m, 1H), 4.26 (dd, *J* = 8.1, 3.8 Hz, 1H), 4.16 (m, 1H), 4.07 (t, *J* = 4.9 Hz, 1H), 3.67–3.63 (m, 1H), 3.62–3.58 (m, 1H); ¹³C NMR (125 MHz, CD₃OD): δ 160.69, 157.50, 152.47, 146.08, 143.93, 138.11, 137.91, 137.67, 128.06, 127.98, 127.92, 127.77, 127.72, 127.48, 127.39, 127.28, 83.00, 81.82, 77.46, 77.29, 73.05, 71.89, 71.76, 69.71.

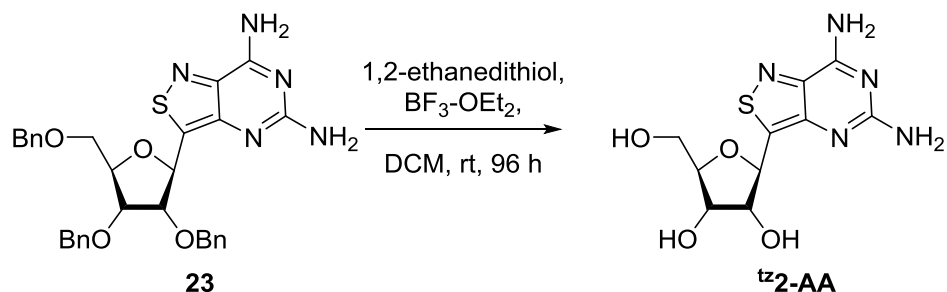


Methyl 3-((2R,3S,4S,5R)-3,4-bis(benzyloxy)-5-((benzyloxy)methyl)tetrahydrofuran-2-yl)-7-imino-5-oxo-4,5-dihydroisothiazolo[4,3-d]pyrimidine-6(7H)-carboxylate (26). In a 50 mL round bottom flask with stir bar, the benzylated isothiazole amide precursor **18b** (1.7 g, 3.12 mmol) was dissolved in anhydrous acetonitrile stirring at room temperature under argon. Ethoxycarbonyl isothiocyanate (0.51 mL, 4.36 mmol) was added dropwise and left to stir 5 hours. After 5 hours stirring at room temperature, EDCI (0.90 g, 4.67 mmol) and hexamethyldisilazane (6.53 mL, 31.2 mmol) were added and the reaction was left to stir at room temperature. After 72 hours, the solution was evaporated to near-dryness and partitioned between EtOAc

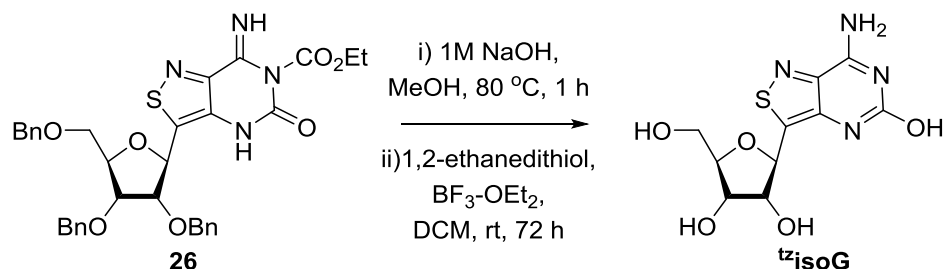
and water. The organic solution was washed twice with aqueous HCl (1M, 5 mL) followed by saturated NaHCO₃ solution. The organic solution was then washed with brine and dried over Na₂SO₄. The solution was evaporated to dryness and subjected to purification by column chromatography (0% EtOAc to 50% EtOAc in Hexanes) to yield a white powder (0.65 g, 33%). R_f 0.44 in 60/40 Hexanes/EtOAc. ¹H NMR (500 MHz, CDCl₃): δ 9.80 (s, 1H), 7.74 (s, 1H), 7.40–7.16 (15H), 5.34 (d, *J* = 7.4 Hz, 1H), 4.65 (d, *J* = 11.8 Hz, 1H), 4.60–4.47 (m, 4H), 4.44 (d, *J* = 11.8 Hz, 1H), 4.36 (dd, *J* = 5.8, 2.8 Hz, 2H), 4.22 (m, 2H), 4.01 (dd, *J* = 4.6, 2.8 Hz, 1H), 3.92 (dd, *J* = 7.4, 4.8 Hz, 1H), 3.60 (dd, *J* = 10.5, 3.4 Hz, 1H), 3.53 (dd, *J* = 10.5, 3.4 Hz, 1H), 1.33 (t, *J* = 7.1 Hz, 3H); ¹³C NMR (125 MHz, CDCl₃): δ 161.93, 153.72, 150.77, 138.18, 137.62, 137.35, 136.81, 131.34, 128.49, 128.47, 128.39, 128.27, 128.22, 128.18, 128.05, 127.89, 127.70, 112.56, 83.36, 83.09, 77.19, 77.01, 73.60, 72.47, 72.09, 69.96, 62.92, 14.18; ESI-HRMS calcd for [C₃₄H₃₃N₄O₇S]⁻ [M-H]⁻ 641.2075, found 641.2077.



3-((2R,3S,4R,5R)-3,4-dihydroxy-5-(hydroxymethyl)tetrahydrofuran-2-yl)isothiazolo[4,3-d]pyrimidine-5,7(4H,6H)-dione (^{tzX}). In a 10 mL round bottom flask with stir bar, the benzylated derivative **22** (0.07 g, 0.12 mmol) was dissolved in anhydrous DCM (2.45 mL) followed by 1,2-ethanedithiol (0.31 mL, 3.67 mmol) and dropwise BF₃·OEt₂ (0.39 mL, 3.06 mmol) and left to stir at room temperature for 72 hours. An aliquot of the reaction was taken and checked using mass chromatography to identify full deprotection of the material. The solution was then evaporated to near-dryness and the resulting residue was subjected to purification by column chromatography (0% MeOH to 20% MeOH in DCM) to yield a white solid (25 mg, 68%). ¹H NMR (500 MHz, CD₃OD): δ 5.15 (d, *J* = 7.0 Hz, 1H), 4.23 – 4.07 (m, 3H), 3.82 (dd, *J* = 11.7, 3.1 Hz, 1H), 3.77 (dd, *J* = 11.7, 3.1 Hz, 1H); ¹³C NMR (125 MHz, CD₃OD): δ 157.30, 150.91, 147.35, 146.60, 134.73, 86.61, 77.20, 77.03, 72.27, 61.62; ESI-HRMS calcd for [C₁₀H₁₀N₃O₆S]⁻ [M-H]⁻ 300.0296, found 300.0296.

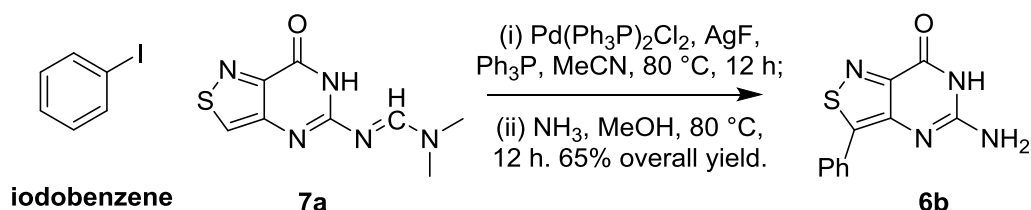


(2R,3S,4R,5R)-2-(5,7-diaminoisothiazolo[4,3-d]pyrimidin-3-yl)-5-(hydroxymethyl)tetrahydrofuran-3,4-diol (tz2-AA). In a 10 mL round bottom flask with stir bar, the benzylated derivative **23** (35 mg, 0.06 mmol) was dissolved in anhydrous DCM (1.2 mL) followed by 1,2-ethanedithiol (0.15 mL, 1.84 mmol) and dropwise $\text{BF}_3\text{-OEt}_2$ (0.19 mL, 1.54 mmol) and left to stir at room temperature for 96 hours. An aliquot of the reaction was taken and checked using mass chromatography to identify full deprotection of the material. The solution was then evaporated to near-dryness and the resulting residue was subjected to purification by reverse phase HPLC ($\text{H}_2\text{O}/\text{MeCN}$ and 0.1% TFA in each solvent, with a gradient from 0 to 11% MeCN over 20 minutes) to yield a white foam (10 mg, 54%). ^1H NMR (500 MHz, D_2O): δ 5.36 (d, $J = 6.3$ Hz, 1H), 4.31 – 4.20 (m, 3H), 3.89 (dd, $J = 23.9, 3.5$ Hz, 1H), 3.85 (dd, $J = 23.9, 3.5$ Hz, 1H); ^{13}C NMR (125 MHz, CD_3OD): δ 158.09, 155.59, 149.32, 141.70, 132.81, 85.61, 77.04, 76.66, 71.27, 61.25. ESI-HRMS calcd for $[\text{C}_{10}\text{H}_{10}\text{N}_3\text{O}_6\text{S}]^+$ $[\text{M}+\text{H}]^+$ 300.0761, found 300.0760.



7-amino-3-((2R,3S,4R,5R)-3,4-dihydroxy-5-(hydroxymethyl)tetrahydrofuran-2-yl)isothiazolo[4,3-d]pyrimidin-5(4H)-one (tzisoG). To a 25 mL round bottom flask with condenser containing the carbamate-protected substrate **26** (0.55 g, 0.86 mmol), MeOH (10.70 mL) was added and the reaction was stirred at room temperature followed by dropwise sodium hydroxide (6.85 mL, 0.25 M) and left to stir under reflux conditions for 1 hour. The material was then evaporated to dryness and partitioned between EtOAc and saturated aqueous ammonium chloride solution. The aqueous solution was washed several times with EtOAc and the organic solution was washed with saturated bicarbonate solution and brine followed by drying over Na_2SO_4 and evaporated to dryness. The resulting residue (0.45 g, 0.79 mmol) was placed under high-vacuum and flushed with argon several times before being dissolved in anhydrous DCM (7.80 mL) stirring with addition of 1,2-ethanedithiol (1.99 mL, 23.66 mmol) and dropwise $\text{BF}_3\text{-OEt}_2$ (2.49 mL, 19.71

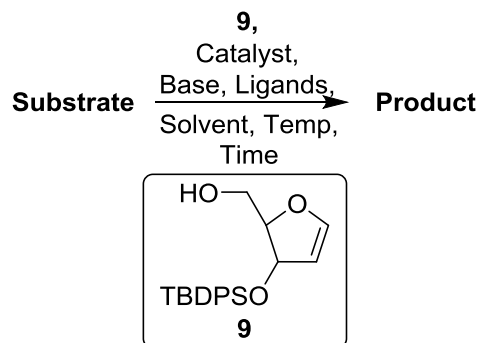
mmol). The flask was placed under argon and left to stir for 72 hours. An aliquot of the reaction was taken and checked using mass chromatography to identify full deprotection of the material. The solution was then evaporated to near-dryness and the resulting residue was subjected to purification by column chromatography (DCM/MeOH with a gradient from 0% to 20% MeOH) to yield a white solid (0.12 g, 51%). ¹H NMR (500 MHz, CD₃OD): δ 5.15 (d, *J* = 7.1 Hz, 1 H), 4.17 (m, 2H), 4.12 (dd, *J* = 5.1, 2.9, 1H), 3.82 (dd, *J* = 11.7, 3.0 Hz, 1H), 3.77 (dd, *J* = 11.7, 3.0 Hz, 1H); ¹³C NMR (125 MHz, CD₃OD): δ 157.95, 157.27, 146.42, 141.62, 135.42, 86.63, 77.22, 77.04, 72.30, 61.65; ESI-HRMS calcd for [C₁₀H₁₁N₄O₅S]⁻ [M-H]⁻ 299.0456, found 299.0454.



Scheme S1. Palladium coupling of **7a** to form benzylated nucleobase (**6b**).

5-amino-3-phenylisothiazolo[4,3-d]pyrimidin-7(6H)-one (6b). To a flame-dried 8 mL reaction vial with stir bar, DMF-protected nucleobase **7a** (0.04g, 0.09 mmol) was dissolved in anhydrous acetonitrile (1.80 mL) followed by addition of palladium bis(triphenylphosphine)dichloride (25 mg, 36 μmol), triphenylphosphine (14 mg, 54 μmol), silver carbonate (99 mg, 0.36 mmol), and iodobenzene (40 μL, 0.36 mmol). The vial was flushed with argon and sealed to stir at 80 °C for 1 hour until starting material was fully consumed as monitored by TLC. The reaction was partitioned between EtOAc and water for extraction. The aqueous solution was washed several times with EtOAc and the organic solution was washed with brine followed by drying over Na₂SO₄. The mixture was used crude and redissolved in a reaction vial with MeOH followed by bubbling ammonia at 0 °C. The vial was sealed and brought to 80 °C for 12 hours. After the reaction was complete, the vial was cooled and solvent evaporated. The resulting residue was purified by column chromatography (DCM/MeOH 95/5) to yield a white solid (0.03 g, 66%). *R_f* 0.63 in 10% MeOH in DCM. ¹H NMR (500 MHz, DMSO-*d*₆): δ 11.20 (br s, 1H), 8.10 (m, 2H), 7.49 (m, 2H), 7.21 (m, 1H), 6.53 (br s, 2H); ¹³C NMR (125 MHz, DMSO-*d*₆): δ 156.70, 152.08, 150.69, 150.09, 146.52, 130.92, 129.45, 129.28, 127.30. ESI-HRMS calcd for [C₁₁H₇N₄OS]⁻ [M-H]⁻ 243.0346, found 243.0344.

Table S1. Palladium coupling trials



| Substrate | Catalyst | Additives | Conditions |
|------------|--|---|----------------------------------|
| 3b, 7b, 8b | Pd(OAc) ₂ | Bu ₄ NBr, NaHCO ₃ | DMF, 50 °C, 10 h |
| | Pd(PPh ₃) ₄ | Bu ₃ N | Dioxane, 70 °C, 10 h |
| | Pd(OAc) ₂ | PPh ₃ , TEA | Dioxane, 100 °C, 10 h |
| | Pd(OAc) ₂ | AsPh ₃ , NaHCO ₃ | DMF, 60 °C, 10 h |
| | Pd(Ph ₃ P) ₂ Cl ₂ | Ag ₂ CO ₃ , Ph ₃ P | MeCN, 80 °C, 12 h |
| | Pd(Ph ₃ P) ₂ Cl ₂ (Pd) ₂ (dba) ₃ | Ag ₂ CO ₃ , AsPh ₃ PPh ₃ | 80 °C, 12 h MeCN, 80 °C, 12 h |

3. Structural analysis

3.1. Experimental summary

The single crystal X-ray diffraction studies were carried out on a Bruker D8 Pt 135 CCD diffractometer equipped with Cu K $_{\alpha}$ radiation ($\lambda = 1.5478$). A 0.220 x 0.050 x 0.050 mm piece of a yellow needle was mounted on a Cryoloop with Paratone oil.

Data were collected in a nitrogen gas stream at 100(2) K using ϕ and ω scans. Crystal-to-detector distance was 45 mm using variable exposure time (5,10 and 20s) depending on θ with a scan width of 1.25°. Data collection was 99.3% complete to 67.50° in θ .

All nonhydrogen atoms were refined anisotropically by full-matrix least-squares (SHELXL-2014). All carbon bonded hydrogen atoms were placed using a riding model. Their positions were constrained relative to their parent atom using the appropriate HFIX command in SHELXL-2014. All other hydrogen atoms (H-bonding) were located in the difference map (N-H).

3.2. X-ray crystal structures

Table S1. Crystal data and structure refinement for **7b**

| | | |
|-----------------------------------|---|--------------------|
| Report date | 2016-04-01 | |
| Identification code | tor91 | |
| Empirical formula | C ₈ H ₈ Br N ₅ O S | |
| Molecular formula | C ₈ H ₈ Br N ₅ O S | |
| Formula weight | 302.16 | |
| Temperature | 100.0 K | |
| Wavelength | 1.54178 Å | |
| Crystal system | Monoclinic | |
| Space group | P 1 21/n 1 | |
| Unit cell dimensions | a = 15.3538(6) Å | α = 90°. |
| | b = 4.3958(2) Å | β = 112.3510(10)°. |
| | c = 17.1443(6) Å | γ = 90°. |
| Volume | 1070.18(7) Å ³ | |
| Z | 4 | |
| Density (calculated) | 1.875 Mg/m ³ | |
| Absorption coefficient | 6.976 mm ⁻¹ | |
| F(000) | 600 | |
| Crystal size | 0.22 x 0.05 x 0.05 mm ³ | |
| Crystal color, habit | yellow needle | |
| Theta range for data collection | 3.295 to 70.194°. | |
| Index ranges | -18 ≤ h ≤ 17, -5 ≤ k ≤ 5, -20 ≤ l ≤ 20 | |
| Reflections collected | 16519 | |
| Independent reflections | 2020 [R(int) = 0.0421] | |
| Completeness to theta = 67.500° | 99.3 % | |
| Absorption correction | Semi-empirical from equivalents | |
| Max. and min. transmission | 0.5220 and 0.3484 | |
| Refinement method | Full-matrix least-squares on F ² | |
| Data / restraints / parameters | 2020 / 0 / 151 | |
| Goodness-of-fit on F ² | 1.079 | |
| Final R indices [I > 2σ(I)] | R1 = 0.0218, wR2 = 0.0555 | |
| R indices (all data) | R1 = 0.0227, wR2 = 0.0562 | |
| Extinction coefficient | n/a | |
| Largest diff. peak and hole | 0.349 and -0.338 e.Å ⁻³ | |

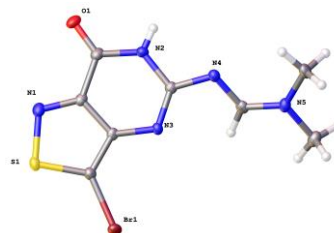


Table S2. Crystal data and structure refinement for **⁴²X**

| | | |
|-----------------------------------|---|-----------------------------|
| Report date | 2016-06-26 | |
| Identification code | Tor111-Tz-Xan | |
| Empirical formula | C10 H11 N3 O6 S | |
| Molecular formula | C10 H11 N3 O6 S | |
| Formula weight | 301.28 | |
| Temperature | 100.0 K | |
| Wavelength | 1.54178 Å | |
| Crystal system | Monoclinic | |
| Space group | P 1 21 1 | |
| Unit cell dimensions | a = 6.8159(3) Å | $\alpha = 90^\circ$. |
| | b = 9.9720(5) Å | $\beta = 98.748(2)^\circ$. |
| | c = 17.7839(8) Å | $\gamma = 90^\circ$. |
| Volume | 1194.68(10) Å ³ | |
| Z | 4 | |
| Density (calculated) | 1.675 Mg/m ³ | |
| Absorption coefficient | 2.752 mm ⁻¹ | |
| F(000) | 624 | |
| Crystal size | 0.25 x 0.17 x 0.1 mm ³ | |
| Crystal color, habit | colorless block | |
| Theta range for data collection | 2.514 to 68.650°. | |
| Index ranges | -8<=h<=8, -11<=k<=11, -21<=l<=21 | |
| Reflections collected | 31295 | |
| Independent reflections | 6325 [R(int) = 0.0498] | |
| Completeness to theta = 67.679° | 98.7 % | |
| Absorption correction | Semi-empirical from equivalents | |
| Max. and min. transmission | 0.821 and 0.645 | |
| Refinement method | Full-matrix least-squares on F ² | |
| Data / restraints / parameters | 6325 / 1 / 368 | |
| Goodness-of-fit on F ² | 1.110 | |
| Final R indices [I>2sigma(I)] | R1 = 0.0307, wR2 = 0.0866 | |
| R indices (all data) | R1 = 0.0312, wR2 = 0.0868 | |
| Absolute structure parameter | 0.046(8) | |
| Extinction coefficient | n/a | |
| Largest diff. peak and hole | 0.222 and -0.239 e.Å ⁻³ | |

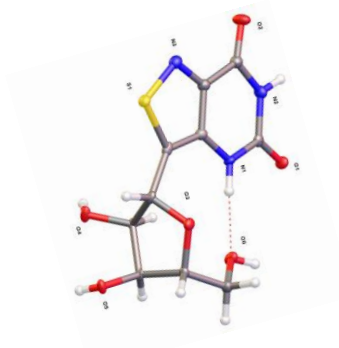
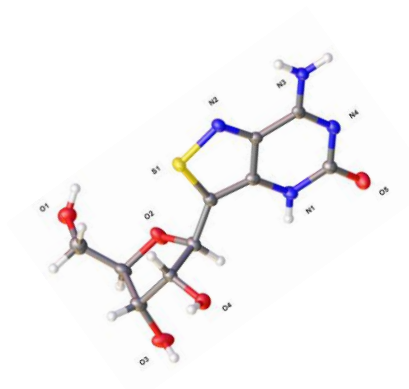


Table S3. Crystal data and structure refinement for *tzIsoG*

| | | |
|-----------------------------------|---|---|
| Report date | 2016-05-16 | |
| Identification code | Tz-IsoG | |
| Empirical formula | C10 H15.50 N4 O6.75 S | |
| Molecular formula | C10 H12 N4 O5 S, 1.75(H2O) | |
| Formula weight | 331.82 | |
| Temperature | 100.0 K | |
| Wavelength | 1.54178 Å | |
| Crystal system | Triclinic | |
| Space group | P1 | |
| Unit cell dimensions | a = 8.0883(2) Å b = 10.9716(3) Å c = 16.0771(4) Å | $\alpha = 72.0700(10)^\circ$ $\beta = 80.2730(10)^\circ$ $\gamma = 86.279(2)^\circ$ |
| Volume | 1337.78(6) Å ³ | |
| Z | 4 | |
| Density (calculated) | 1.648 Mg/m ³ | |
| Absorption coefficient | 2.578 mm ⁻¹ | |
| F(000) | 694 | |
| Crystal size | 0.234 x 0.116 x 0.095 mm ³ | |
| Crystal color, habit | Colorless Blade | |
| Theta range for data collection | 2.925 to 68.267° | |
| Index ranges | -9<=h<=9, -13<=k<=13, -19<=l<=19 | |
| Reflections collected | 47934 | |
| Independent reflections | 9070 [R(int) = 0.0321] | |
| Completeness to theta = 68.000° | 97.1 % | |
| Absorption correction | Semi-empirical from equivalents | |
| Max. and min. transmission | 0.3200 and 0.2197 | |
| Refinement method | Full-matrix least-squares on F ² | |
| Data / restraints / parameters | 9070 / 3 / 817 | |
| Goodness-of-fit on F ² | 1.025 | |
| Final R indices [I>2sigma(I)] | R1 = 0.0286, wR2 = 0.0758 | |
| R indices (all data) | R1 = 0.0311, wR2 = 0.0773 | |
| Absolute structure parameter | 0.036(5) | |
| Extinction coefficient | n/a | |
| Largest diff. peak and hole | 0.317 and -0.181 e.Å ⁻³ | |



3.3. ¹²X Crystal structure overlay

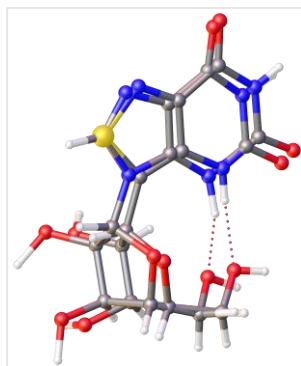


Figure S1. Overlay of ¹²X crystal structure and previously published anhydrous xanthosine crystal structure.^{S5}

4. Absorption and emission spectroscopy

Table S4. Photophysical and chemical properties of isothiazolo[4,3-*d*]pyrimidine nucleoside analogs

| | solvent | $\lambda_{\text{abs}} (\epsilon)^a$ | $\lambda_{\text{em}} (\Phi)^a$ | $\Phi\epsilon$ | Stokes shift ^a | polarity sensitivity ^b | abs | pK_a^c | em |
|------------------------|---------|-------------------------------------|--------------------------------|----------------|---------------------------|-----------------------------------|------------------------|-------------------------|----|
| tzisoG | water | 334 (9.14±0.03) | 413 (0.047±0.004) | 365 | 5.73±0.04 | 20±1 | 3.4±0.1 | 3.90±0.01 | |
| | dioxane | 342 (8.6±0.1) | 416 (0.034±0.006) | 345 | 5.21±0.04 | | 11.5±0.1 | 11.20±0.01 | |
| tzX | water | 321 (6.61±0.07) | 472 (0.043±0.003) | 264 | 10.03±0.02 | 61±2 3.0±0.8 | 9.03±0.05 | 1.98±0.01 8.5±0.2 | |
| | dioxane | 320 (6.60±0.03) | 384 (0.003±0.001) | 13 | 5.10±0.05 | | | | |
| tz2-AA | water | 346 (2.85±0.07) | 447 (0.27±0.03) | 712 | 7.52±0.05 | 140±2 | 6.91±0.01 | 2.55±0.01 5.93±0.02 | |
| | dioxane | 349 (3.08±0.02) | 468 (0.22±0.02) | 616 | 6.24±0.01 | | | | |
| tzA^d | water | 338 (7.79±0.09) | 410 (0.053±0.004) | 413 | 5.23±0.06 | 28±2 | 4.25±0.05 | 3.29±0.03 | |
| | dioxane | 342 (7.42±0.04) | 409 (0.026±0.002) | 193 | 4.76±0.02 | | | | |
| tzC^d | water | 325 (5.4±0.1) | 411 (0.053±0.005) | 289 | 6.42±0.06 | 10±1 | 2.9±0.2 | 2.46±0.06 10.38±0.05 | |
| | dioxane | 333 (5.03±0.02) | 419 (0.036±0.003) | 181 | 6.14±0.03 | | | | |
| tzG^d | water | 333 (4.87±0.04) | 459 (0.24±0.02) | 1203 | 8.27±0.06 | 102±7 | 3.55±0.03 8.51±0.02 | 9.88±0.07 | |
| | dioxane | 339 (4.65±0.08) | 425 (0.17±0.01) | 539 | 6.01±0.05 | | | | |
| tzI^d | water | 316 (7.6±0.2) | 377 (0.006±0.001) | 46 | 5.13±0.05 | 12.7±0.5 | 9.26±0.03 | 7.83±0.01 | |
| | dioxane | 315 (6.6±0.1) | 372 (0.004±0.001) | 26 | 4.79±0.04 | | | | |
| tzU^d | water | 312 (5.17±0.06) | 392 (0.008±0.001) | 41 | 6.53±0.02 | 45±4 | 2.2±0.1 8.88±0.08 | 8.9±0.1 | |
| | dioxane | 314 (5.2±0.1) | 377 (0.004±0.001) | 21 | 5.36±0.07 | | | | |

^a λ_{abs} , ϵ , λ_{em} and Stokes shift are reported in nm, $10^3 \text{ M}^{-1} \text{ cm}^{-1}$, nm and 10^3 cm^{-1} respectively. All the photophysical values reflect the average over three independent measurements. ^b Sensitivity to solvent polarity reported in $\text{cm}^{-1}/(\text{kcal mol}^{-1})$ is equal to the slope of the linear fit in Figure 5b. ^c pK_a reflect the average over three independent measurements and are equal to the inflection point determined by the fitting curves in Figure 5c and 5d. ^d From previous work.^{S1}

4.1. General

Spectroscopic grade DMSO and dioxane were obtained from Sigma Aldrich and aqueous solutions were prepared with de-ionized water. All the measurements were carried out in a 1 cm four-sided quartz cuvette from Helma.

Absorption spectra were measured on a Shimadzu UV-2450 spectrophotometer setting the slit at 1 nm and using a resolution of 0.5 nm. All the spectra were corrected for the blank. Steady state emission spectra were measured on a Horiba Fluoromax-4 equipped with a cuvette holder with a stirring system setting both the excitation and the emission slits at 3 nm, the resolution at 1 nm and the integration time 0.1 s. The probe was excited just before the absorbance maxima to provide enough energy to excite all the fluorophore population, and maximize the recorded emission signal.

All the spectra were corrected for the blank. Both instruments were equipped with a thermostat controlled ethylene glycol-water bath fitted to specially designed cuvette holder and the temperature was kept at 25.0 ± 0.1 °C.

Nucleosides were dissolved in DMSO to prepare highly concentrated stock solutions: ¹²⁵IsoG (3.33 mM), ¹²⁵X (3.32 mM) and ¹²⁵2-AA (3.34 mM). In a typical experiment, aliquots (10 μl) of the concentrated DMSO solution were diluted with air-saturated solvents (3 mL). The solutions were mixed with a pipette for 10 seconds and placed in the cuvette holder at 25.0 ± 0.1 °C for 3 minutes before spectra were recorded. All sample contain 0.3 v/v % of DMSO.

4.2. Fluorescence quantum yield

The sample concentrations were adjusted to have an absorbance lower than 0.1 at the excitation wavelength (λ_{ex}). The fluorescence quantum yield (Φ) were evaluated based on an external standard, 2-aminopurine (0.68 in water, λ_{ex} 320 nm) by using the following equation.

$$\Phi = \Phi_{STD} \frac{I}{I_{STD}} \frac{Abs_{STD}}{Abs} \frac{n^2}{n_{STD}^2}$$

Where Φ_{STD} is the fluorescence quantum yield of the standard, I and I_{STD} are the integrated area of the emission band of the sample and the standard respectively, Abs and Abs_{STD} are the absorbance at the excitation wavelength for the sample and the standard respectively and n and n_{STD} are the solvent refractive index of the sample and the standard solutions respectively.

4.3. Sensitivity to pH

Aqueous stock solutions (100 mL) were prepared by mixing aqueous sodium phosphate monobasic (0.5 M), aqueous sodium phosphate dibasic (0.5 M) and aqueous sodium chloride (2 M) to have a final concentration of 100 mM NaCl and 10 mM phosphate ions. The pH of each solution was adjusted to the desire value by adding aliquots of 2 M aqueous HCl or 2 M aqueous NaOH prior to spectral measurements.

The absorption (λ_{abs}) and the emission (λ_{em}) maxima were plotted versus the pH and fitted using a Boltzmann sigmoidal curve using Kaleidagraph 3.5. The pK_a values were determined by interpolation of the fitting curves. The reported pK_a values represent the average of three independent sets of measurements per each nucleoside. The values and the relative standard deviations are reported in table S4.

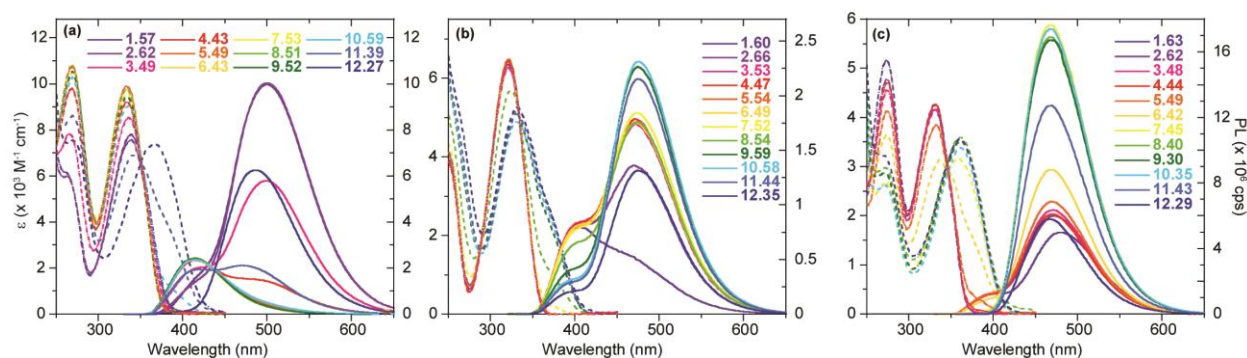


Figure S2. Absorption (dashed lines) and emission (solid lines) traces in buffer solutions at different pH for ¹³C-isoG (a), ¹³C-X (b) and ¹³C-2-AA (c). The emission spectra were normalized to 0.1 intensity at the excitation wavelength.

Emission and the corresponding excitation spectra were also recorded, at specific pH (acidic, neutral and basic), varying the excitation wavelength or the emission wavelength of interest. The aqueous solution of ¹³C-isoG, ¹³C-X or ¹³C-2-AA at specific pH were prepared as described above. The emission spectra were recorded upon excitation every 20 nm covering the main absorption band (e.g. 390, 370 to 270 nm). The emission spectra were finally corrected by the corresponding intensity at the excitation wavelength or normalized to unit in intensity at the emission maxima. The excitation spectra were recorded upon fixing the emission wavelength of interest with a pathway of 20 nm covering all the emission spectra (e.g. 650, 630 to 370 nm). The excitation spectra were finally normalized to unit in intensity at the excitation maxima.

Note that for Tables 4 and S4, the number of pKa values differs between absorption and emission in some cases. The reported pKa values were determined based on the experimental shift (energy variation) of the absorption and/or emission maxima as a function of pH. A priori, a protonation/deprotonation equilibrium might have a more pronounced effect on the energy of ground state of a molecule rather than on its excited state or vice versa. This would be expected to result in a shift of the absorption or the emission maxima. In addition, if the shift due to the protonation/deprotonation equilibrium is comparable to the sensitivity of the instrument (± 1 nm) it would be not possible to unequivocally and accurately determine a pKa value. Complementary evaluation of the protonation/deprotonation phenomena might be performed by evaluating other parameters such variation in the fluorescence quantum yield or molar extinction coefficient as function of pH.

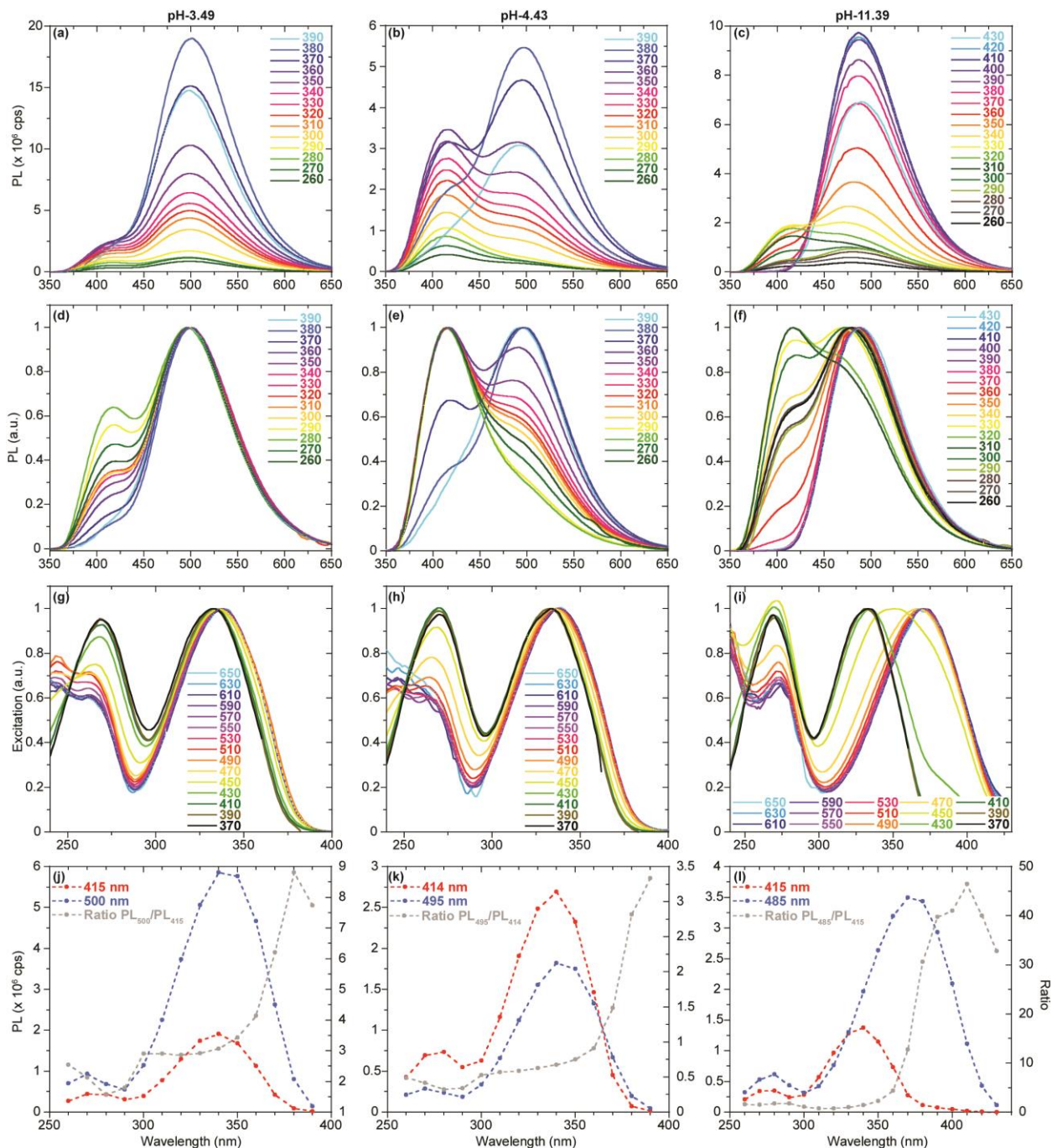


Figure S3. Emission spectra recorded upon excitation at different wavelengths and normalized for the corresponding absorbance intensity (a, b and c) or normalized to unit in intensity (d, e and f) for aqueous solutions of t^2isoG at pH 3.49, 4.43 and 11.39. Excitation spectra normalized to unit (g, h and i) recorded at selected emission spectra wavelengths, covering the whole emission band of aqueous solutions of t^2isoG at pH 3.49, 4.43 and 11.39. Extrapolated excitation spectra by plotting the emission spectra intensities at selected wavelengths upon excitation at different wavelengths (j, k and l) of aqueous solutions of t^2isoG at pH 3.49, 4.43 and 11.39.

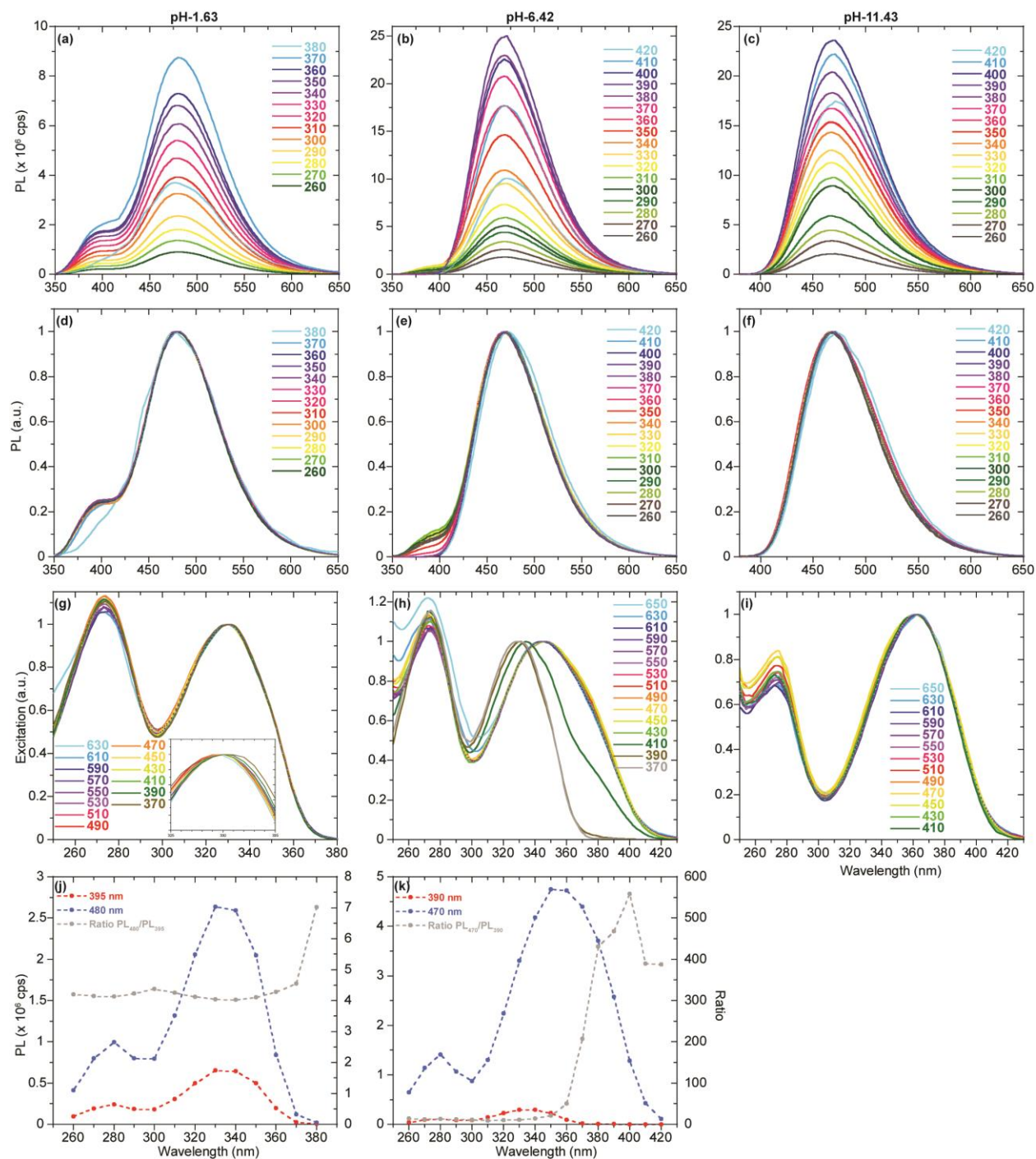


Figure S4. Emission spectra recorded upon excitation at different wavelengths and normalized for the corresponding absorbance intensity (a, b and c) or normalized to unit in intensity (d, e and f) for aqueous solutions of **t²-AA** at pH 1.63, 6.42 and 11.43. Excitation spectra normalized to unit (g, h and i) recorded at selected emission spectra wavelengths, covering the whole emission band of aqueous solutions of **t²-AA** at pH 1.63, 6.42 and 11.43. Extrapolated excitation spectra by plotting the emission spectra intensities at selected wavelengths upon excitation at different wavelengths (j and k) of aqueous solutions of **t²-AA** at pH 1.63 and 6.42.

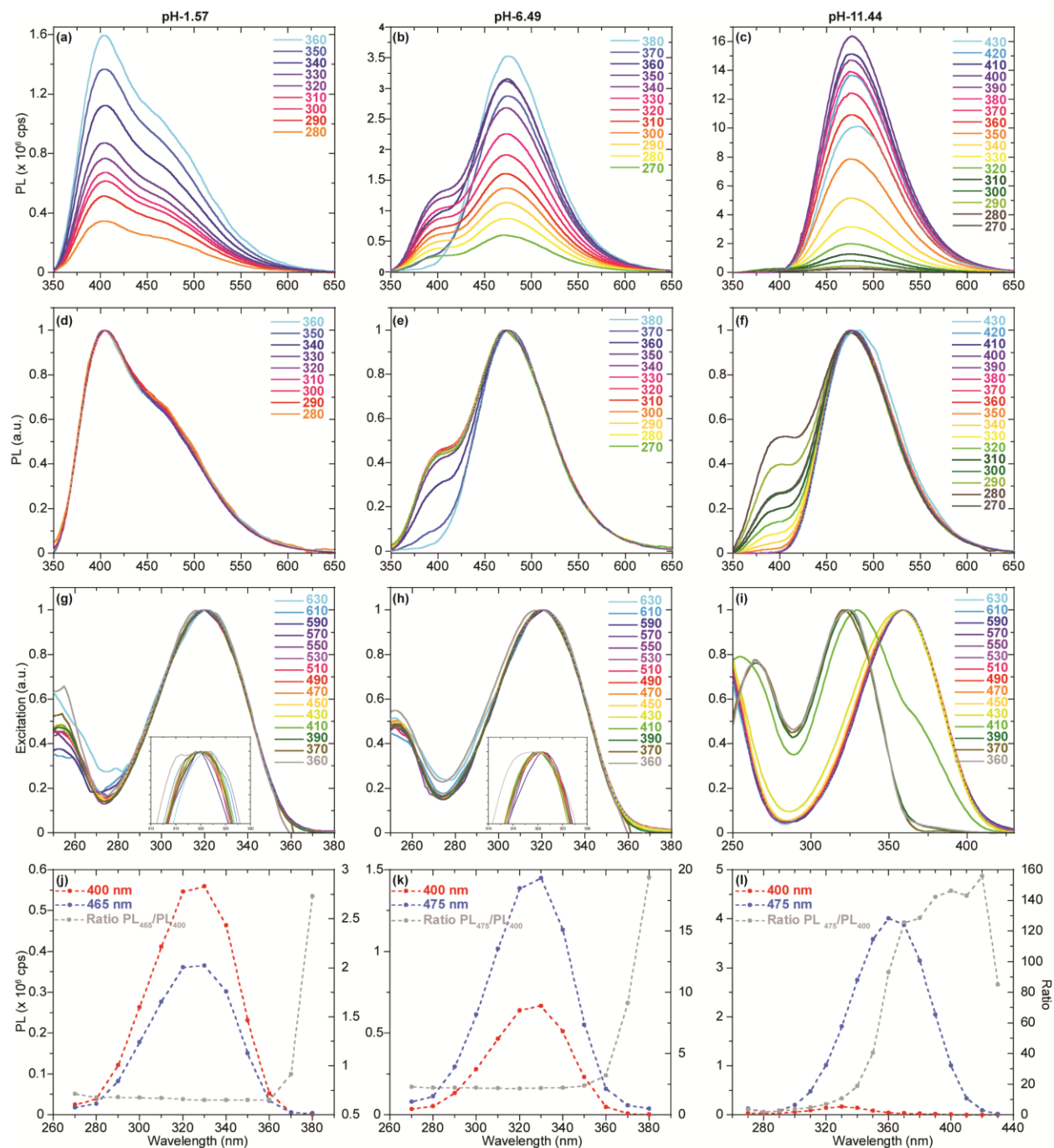


Figure S5. Emission spectra recorded upon excitation at different wavelengths and normalized for the corresponding absorbance intensity (a, b and c) or normalized to unit in intensity (d, e and f) for aqueous solutions of t²X at pH 1.57, 6.49 and 11.44. Excitation spectra normalized to unit (g, h and i) recorded at selected emission spectra wavelengths, covering the whole emission band of aqueous solutions of t²X at pH 1.57, 6.49 and 11.44. Extrapolated excitation spectra by plotting the emission spectra intensities at selected wavelengths upon excitation at different wavelengths (j, k and l) of aqueous solutions of t²X at pH 1.57, 6.49 and 11.44.

Note for Figures S3(j-l), S4(j-k), and S5(j-l) above: These spectra are reconstructed excitation spectra from a series of emission spectra recorded by varying the excitation wavelengths. They have been derived by plotting the relative intensities of the maxima (relative maximum and absolute maximum) as function of the excitation wavelength. The reported spectra are taken for confirmation of the excitation spectra recorded with a standard setup. The plotted ratio (grey) is an indication for potential selective excitation of one of the two present ground states. In most cases (due to the significant overlap of the ground state spectra) this ratio was small and constant over the excitation range. Nevertheless, in some cases (See figures S3l and S5l), because of the remarkable bathochromic shift of one of the ground state in comparison to the other, this ratio showed a significant increment at lower energy excitation.

4.4. Sensitivity to polarity

Experiments evaluating the effect of polarity were performed in water, dioxane and their mixtures (20, 40, 60 and 80 v/v % water in dioxane). The sample $E_T(30)$ values were determined by dissolving a small amount of Reichardt's dye in the mixture of the same solvent used to dilute the nucleoside's DMSO sample. The observed long wavelength absorption maximum (λ_{abs}^{max}) was converted to the $E_T(30)$ values with the following equation.

$$E_T(30) = \frac{28591}{\lambda_{abs}^{max}}$$

Table S5. $E_T(30)$ experimental values for water/dioxane mixtures

| Water % in dioxane | Reported $E_T(30)^a$ (kcal mol ⁻¹) | Experimental $E_T(30)^b$ (kcal mol ⁻¹) | Experimental $E_T(30)^c$ (kcal mol ⁻¹) | Experimental $E_T(30)^d$ (kcal mol ⁻¹) |
|--------------------|---|---|---|---|
| 0 | 36.4 | 36.4 | 36.4 | 36.4 |
| 20 | 48.3 | 48.5 | 48.4 | 48.5 |
| 40 | 51.6 | 52.9 | 51.7 | 52.2 |
| 60 | 55.0 | 55.6 | 54.5 | 55.1 |
| 80 | 57.5 | 57.5 | 56.8 | 58.0 |
| 100 | 63.1 | — | — | — |

^a Literature values.⁵⁶ ^b values for ¹²⁵IsoG titration. ^c values for ¹²⁵X titration. ^d values for ¹²⁵2-AA titration. Due to solubility limitation the water $E_T(30)$ value was not calculated.

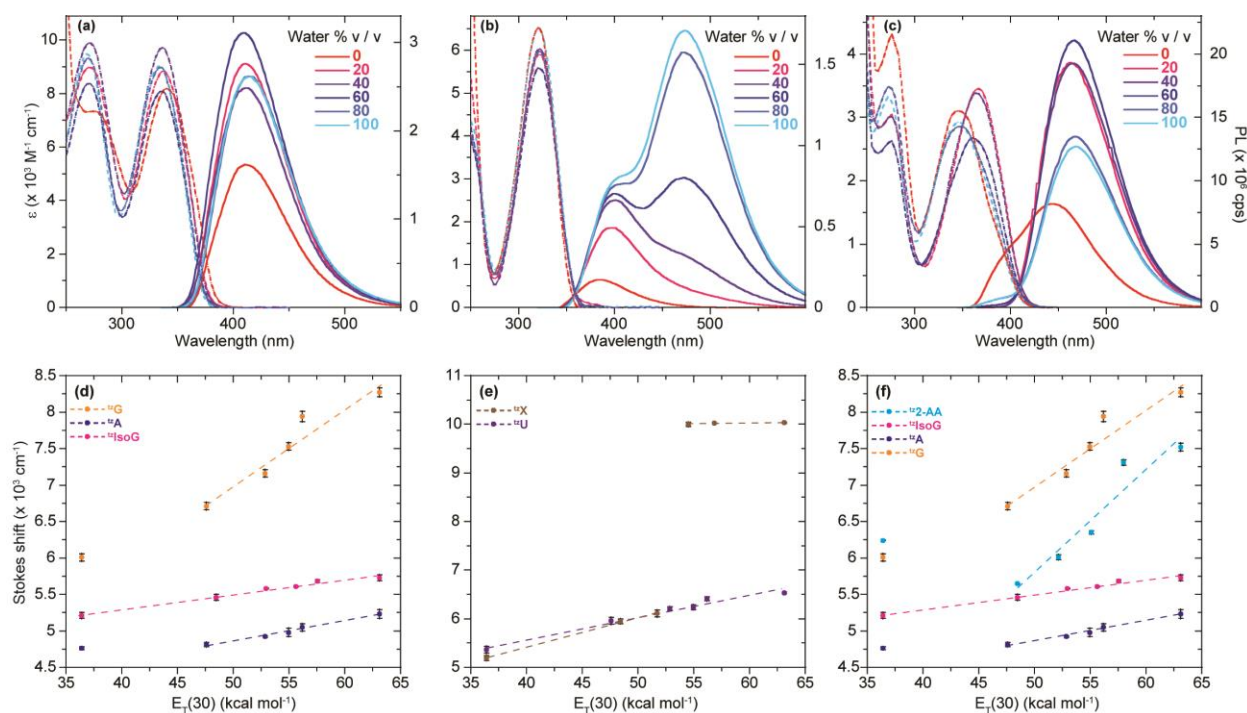


Figure S6. Absorption (dashed lines) and emission (solid lines) traces in water, dioxane and mixture thereof for ¹²⁵isoG (a), ¹²⁵X (b), ¹²⁵2-AA (c). The emission spectra were normalized to 0.1 intensity at the excitation wavelength. Stokes shift correlation versus solvent polarity ($E_T(30)$) of water/dioxane mixtures for ¹²⁵isoG (d), ¹²⁵X (e), ¹²⁵2-AA (f) in comparison to previously reported isothiazolo[4,3-d]pyrimidine-based nucleoside.^{S1}

5. Enzymatic conversion by adenosine deaminase

5.1 General methods

Bovine Spleen ADA was obtained from Sigma Aldrich (EC Number 232-817-5). The commercial solution (1150 U/mL in 3.2 M (NH₄)₂SO₄, 0.01 M potassium phosphate, pH 6.0) was diluted to 3.45 U/mL by dissolving an aliquot (3 μl) in phosphate buffer (997 μl, 50 mM, pH 7.4). The enzyme solution was freshly prepared and kept on ice prior to use.

Concentrated stock solutions in DMSO were prepared for ¹²⁵A (3.52 mM), ¹²⁵2-AA (3.34 mM), **2-AA** (3.54 mM). The reaction solutions were prepared in 1 cm four-sided quartz cuvette from Helma to give a nucleoside and enzyme concentration of 11.7 μM and 27.6 mU/mL in phosphate buffer (50 mM, pH 7.4) and were measured at 25.00 ± 0.10 °C.

5.2. Steady state absorption and emission experiments with adenosine deaminase

Steady state absorption spectra over time were measured on a Shimadzu UV-2450 spectrophotometer setting the slit at 1 nm, using a resolution of 0.5 nm and a time-delay of 30 s. All the spectra were corrected for the blank. Steady state emission spectra were measured on a Horiba Fluoromax-4 equipped with a cuvette holder with a stirring system, setting the excitation and the emission slits at 3 nm, the resolution at

1 nm, integration time 0.1 s and a time-delay of 20 s. The steady state fluorescence spectra were performed upon excitation at 338 nm. All the spectra were corrected for the blank.

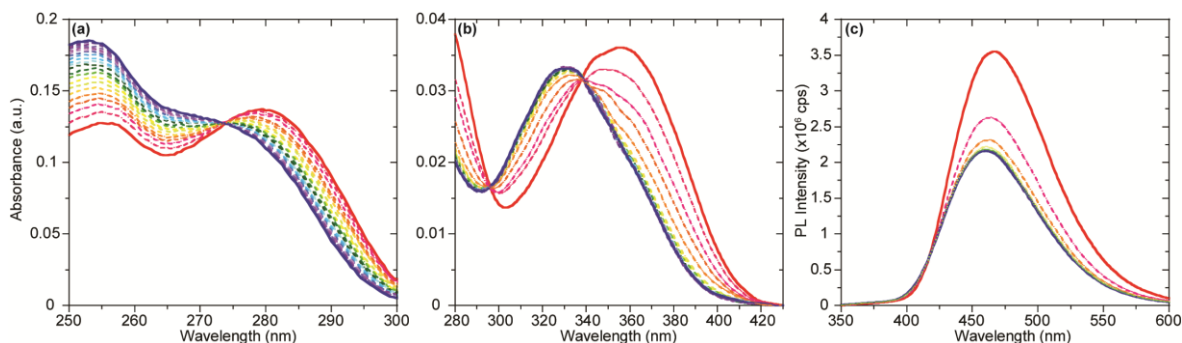


Figure S7. Steady state absorption traces of **2-AA** (a) and **^{tz}2-AA** (b) enzymatic conversion by ADA to **G** and **^{tz}G** over a time range from 0 (solid red) to 600 s (solid blue). (c) Steady state emission traces of **^{tz}2-AA** ADA-mediated conversion to **^{tz}G** from 0 (solid red) to 300 s (solid blue).

The initial rate constant (k_1) and the reaction half-time ($t_{1/2}$) were determined by a semi-logarithmic plot of the signal (absorbance or emission intensity) variation in the first 150 s versus time, assuming a pseudo first-order kinetic for the reaction and using the following equations.

$$\ln[X] = -k_1 t + \ln[X]_0$$

$$t_{1/2} = \frac{\ln(2)}{k_1}$$

Where $[X]$ is the experimental signal over time, $[X]_0$ is the initial signal at time zero, t is time, and k_1 is the slope of the linear trend. The reported values are the average of three independent set of measurements and the coefficient of determination (R^2) for the linearization were higher than 0.99 for the **^{tz}2-AA** trace and higher than 0.97 for **2-AA** trace.

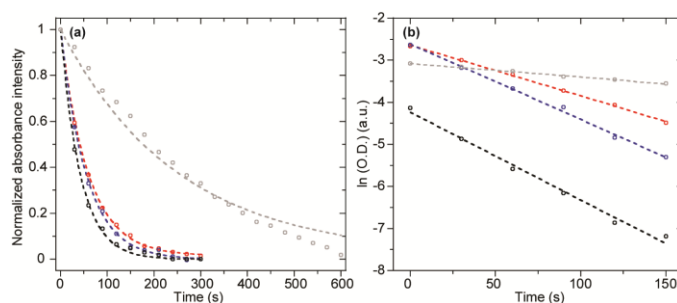


Figure S8. (a) Normalized absorbance intensity signal over time upon addition of ADA for **^{tz}A** (340 nm, blue) and **A** (260 nm, red), **^{tz}2-AA** (370 nm, black) and native **2-AA** (290 nm, grey). (b) Semi-logarithmic plot of the absorbance signal intensity over the first 150 seconds upon addition of ADA for **A** (260 nm, red), **^{tz}A** (340 nm, blue), **^{tz}2-AA** (370 nm, black) and native **2-AA** (290 nm, grey). Data for **A** and **^{tz}A** are taken from previous published results.^{S1}

5.3. Fluorescence based kinetic assays in presence of ADA

The ADA-mediated enzymatic conversion of ^{tz}2-AA to ^{tz}G was also followed by emission spectroscopy by monitoring the emission intensity signal at 475 nm upon excitation at 338 nm (the isosbestic point determined by absorption spectroscopy). Excitation at the isosbestic point gives emission spectra that are unaffected by changes in absorbance. The real-time conversion of ^{tz}2-AA to ^{tz}G was measured on a Horiba Fluoromax-4 equipped with a cuvette holder with a built-in stirring system, setting the excitation and the emission slits at 1 and 3 nm respectively and taking a point every two seconds for 300 seconds upon addition of ADA. The initial rate constant (k_1) and the reaction half-time ($t_{1/2}$) were determined as described above.

Table S7. Enzyme mediated adenosine deaminase initial rate – Photophysical-based assay

| | Absorbance | | | Emission | | |
|---|-------------------|---|--------------------|-----------------------------------|---|--------------------|
| | λ_{mnr}^a | k_1^b (10^{-3} s^{-1}) | $t_{1/2}^c$ (s) | $\lambda_{mnr} (\lambda_{exc})^a$ | k_1^b (10^{-3} s^{-1}) | $T_{1/2}^c$ (s) |
| A to I ^d | 260 | 12.2±0.8 | 57±4 | – | – | – |
| ^{tz} A to ^{tz} I ^d | 340 | 17.9±0.7 | 39±2 | 410 (322) | 20.8±0.4 | 33.3±0.7 |
| 2-AA to G | 290 | 3.3±0.1 | 207±2 | – | – | – |
| ^{tz} 2-AA to ^{tz} G | 370 | 24±1 | 29±1 | 475 (338) | 24.4±0.6 | 28.4±0.5 |

^a λ_{mnr} and λ_{exc} are in nm and represent the followed and the excitation wavelengths respectively in the specific experiment. ^b Pseudo first order reaction kinetic equal to the slope of the linear trend in semi-logarithmic plot of the experimental traces. ^c $t_{1/2}$ is the reaction half-time calculated assuming a pseudo first-order enzymatic kinetic and reflect the average over three independent measurements. ^d Data from previous work.^{S1}

5.4 HPLC analysis for the adenosine deaminase mediated conversion

5.4.1. General

To corroborate the experiments described above, the ADA-mediated deamination was monitored by chromatography. HPLC analysis was carried out with an Agilent 1200 series system with an Eclipse XDB-C18 5 μ m, 4.5 × 150 mm column. 0.1% formic acid stock solutions were prepared by dissolving 1 mL of formic acid (Acros, 99%) in 999 mL HPLC grade acetonitrile (Sigma) or MilliQ water and filtered using Millipore type GNWP 0.2 μ m filters before use. Each injection (40 μ l) was subjected to a gradient (21 minutes, from 0.5 to 10% acetonitrile 0.1% formic acid in water 0.1% formic acid) followed by a flush (5 minutes). A flow rate of 1 mL / minute was used and the run was carried out at 25.00 ± 0.10 °C. Each run was monitored at 260 and 330 nm with calibrated references at 650 nm and slit set at 1 nm.

5.4.2. HPLC analysis for the enzymatic conversion of ^{tz}2-AA to ^{tz}G

Concentrated stock solution of ^{tz}2-AA (5 μ l, 3.34 mM) was diluted with air-saturated phosphate buffer solution (1483 μ l, 50 mM, pH 7.4) and finally ADA (12 μ l, 3.45 U/mL) was added and quickly mixed. The solution was gently stirred while placed in a heating block at 25.00 ± 0.10 °C. Aliquots (100 μ l) of the solution

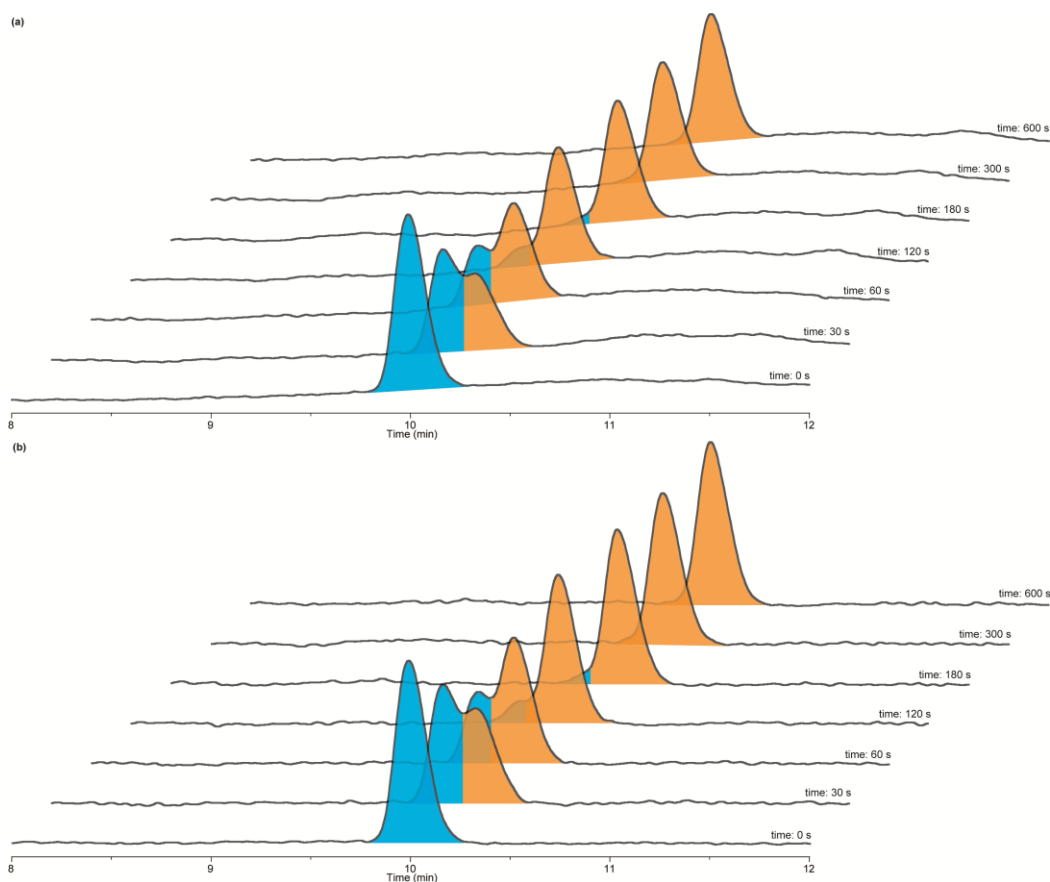
were quenched (after 30, 60, 120, 300 and 600 seconds) by addition of HClO₄ (7 μl, 70% w/w solution) and by placing the sample in dry-ice. Aliquots (40 μl) of the quenched solution were filtered and HPLC analyzed. **SAFETY: Note that an extreme reaction hazard exists between DMSO and perchloric acid. Caution is advised when using these two incompatible reagents together.**

The HPLC traces were corrected for the blank and imported on PeakFit v4.12. The peaks of interest were fitted or deconvoluted and the resulting peak area values were normalized by the extinction coefficient ¹²**2-AA** ($\epsilon_{A-260} = 3.73 \cdot 10^3$ and $\epsilon_{A-330} = 3.97 \cdot 10^3 \text{ M}^{-1} \text{ cm}^{-1}$) and ¹²**G** ($\epsilon_{A-260} = 2.85 \cdot 10^3$ and $\epsilon_{A-330} = 4.26 \cdot 10^3 \text{ M}^{-1} \text{ cm}^{-1}$) in water with 0.1% formic acid and the relative area were plotted as a function of time.

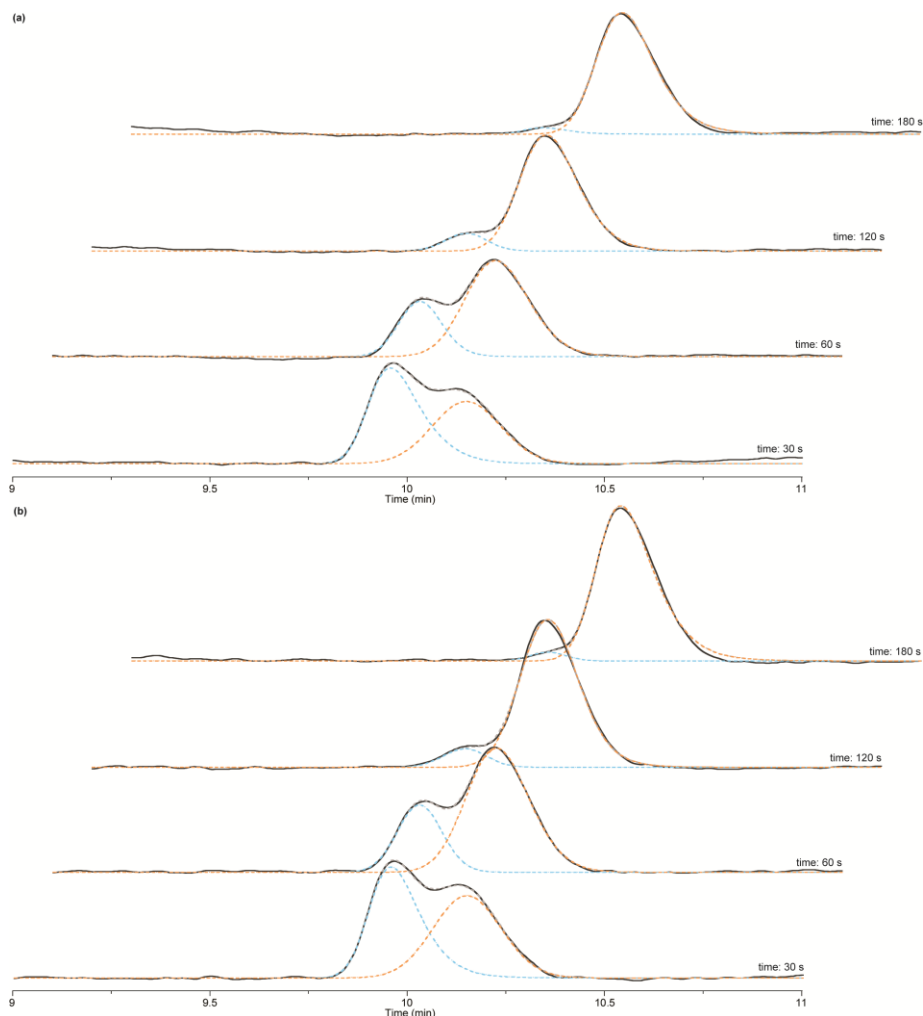
The relative peak areas of the substrate (S) and product (P) were plotted over time. The trend line represents the loss of substrate (S) and the product (P) formation by non-linear regression function over time for a pseudo first-order kinetic reaction according to the following equations:

$$[S] = \{[S]_0 - [S]_\infty\} e^{-k_1 t} + [S]_\infty$$

$$[P] = [P]_\infty (1 - e^{-k_1 t})$$



FigureS9. ADA-mediated deamination analysis by HPLC monitored at 260 (a) and 330 (b) nm. Chromatogram showing the time course of enzymatic conversion of ¹²**2-AA** (cyan) to ¹²**G** (orange). Each set shows six time points following the addition of ADA.



FigureS10. HPLC peaks deconvolution at 260 (a) and 330 (b) nm. Chromatogram showing the time course of enzymatic conversion of $t^2\text{-AA}$ (cyan) to $t^2\text{G}$ (orange). Each time-set shows the observed chromatogram (black solid), the generated signal (grey dashed), the deconvoluted peak for $t^2\text{-AA}$ (cyan dashed) and for $t^2\text{G}$ (dashed orange).

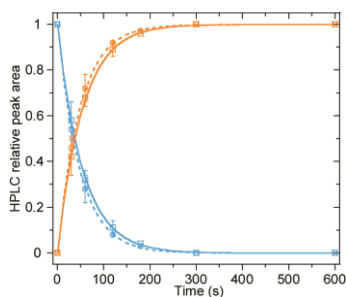
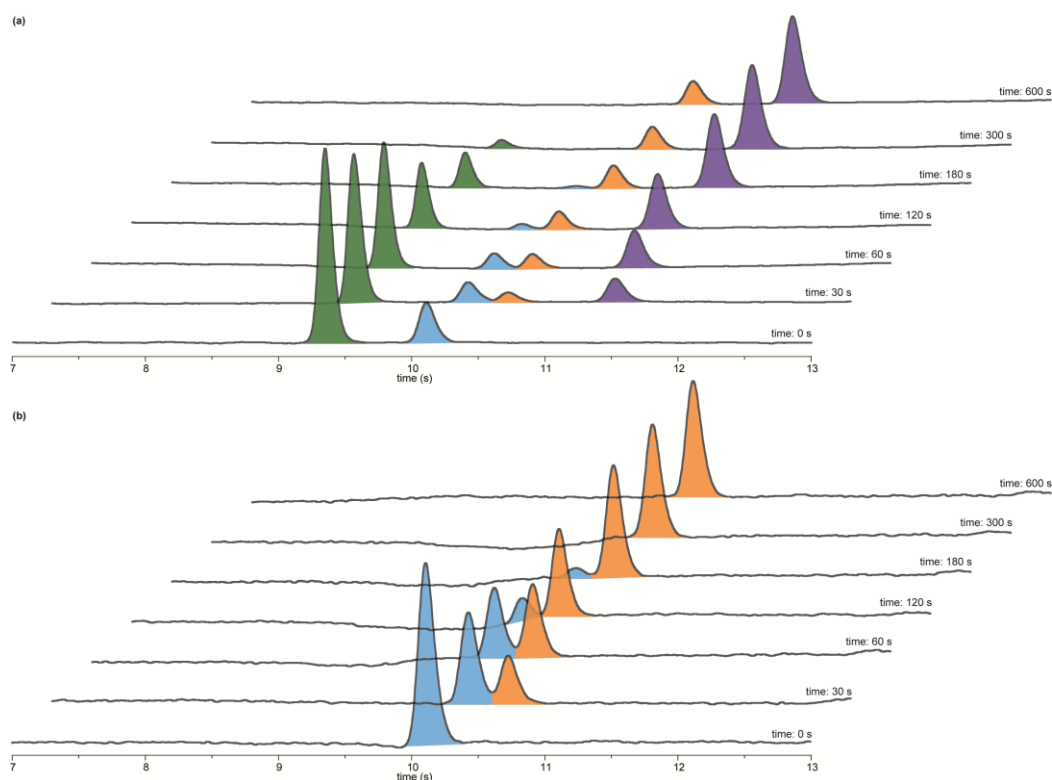


Figure S11. Enzymatic deamination of $t^2\text{-AA}$ (cyan) to provide $t^2\text{G}$ (orange) monitored by HPLC relative peak area variation at different time-points monitored at 260 (dashed) and 330 (solid) nm.

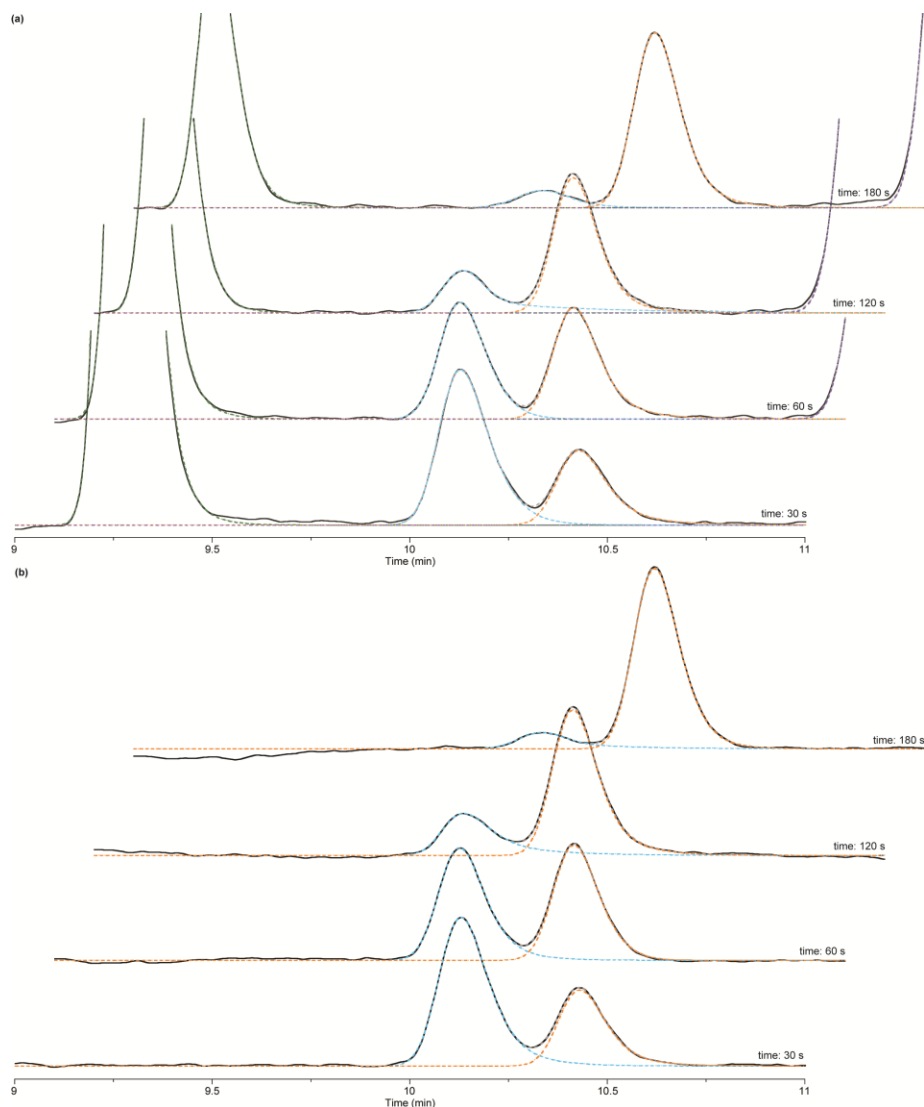
5.5 HPLC analysis for the competitive enzymatic deamination

As a general procedure, concentrated stock solution of ${}^{\text{t}}\mathbf{2-AA}$ (5 μl , 3.34 mM) \mathbf{A} (5 μl , 3.74 mM) were diluted with air-saturated phosphate buffer solution (1478 μl , 50 mM, pH 7.4) and finally ADA (12 μl , 3.45 U/mL) was added and quickly mixed. The solution was gently stirred while placed in a heating block at 25.00 ± 0.10 °C. Aliquots (100 μl) of the solution were quenched (after 30, 60, 120, 300 and 600 seconds) by addition of HClO_4 (7 μl , 70% w/w solution) and by placing the sample in dry-ice. Aliquots (40 μl) of the quenched solution were filtered and HPLC analyzed.

The HPLC traces were corrected for the blank and imported on PeakFit v4.12. The peaks of interest were fitted or deconvoluted and the resulting peak area values were normalized by the extinction coefficient for \mathbf{A} ($\epsilon_{\text{A-260}} = 12.78 \cdot 10^3$), \mathbf{I} ($\epsilon_{\text{I-260}} = 5.67 \cdot 10^3$), ${}^{\text{t}}\mathbf{A}$ ($\epsilon_{\text{A-260}} = 2.69 \cdot 10^3$ and $\epsilon_{\text{A-330}} = 8.86 \cdot 10^3 \text{ M}^{-1} \text{ cm}^{-1}$), ${}^{\text{t}}\mathbf{I}$ ($\epsilon_{\text{A-260}} = 2.84 \cdot 10^3$ and $\epsilon_{\text{A-330}} = 5.05 \cdot 10^3 \text{ M}^{-1} \text{ cm}^{-1}$), ${}^{\text{t}}\mathbf{2-AA}$ ($\epsilon_{\text{A-260}} = 3.73 \cdot 10^3$ and $\epsilon_{\text{A-330}} = 3.97 \cdot 10^3 \text{ M}^{-1} \text{ cm}^{-1}$) and ${}^{\text{t}}\mathbf{G}$ ($\epsilon_{\text{A-260}} = 2.85 \cdot 10^3$ and $\epsilon_{\text{A-330}} = 4.26 \cdot 10^3 \text{ M}^{-1} \text{ cm}^{-1}$) in water with 0.1% formic acid and the relative area were plotted as a function of time.



FigureS12. ADA-mediated competitive deamination analysis by HPLC monitored at 260 (a) and 330 (b) nm. Chromatogram showing the time course of enzymatic conversion of isomolar concentrations of ${}^{\text{t}}\mathbf{2-AA}$ (cyan) and \mathbf{A} (green) converted to ${}^{\text{t}}\mathbf{G}$ (orange) and \mathbf{I} (purple). Each set shows six time points following the addition of ADA.



FigureS13. HPLC peaks deconvolution at 260 (a) and 330 (b) nm. Chromatogram showing the time course of enzymatic competitive conversion of t^2 -AA (cyan) to t^2 G (orange) and **A** (green) to **I** (purple). Each time-set shows the observed chromatogram (black solid), the generated signal (grey dashed), the deconvoluted peak for t^2 -AA (cyan dashed), t^2 G (dashed orange), **A** (dashed green) and **I** (dashed purple).

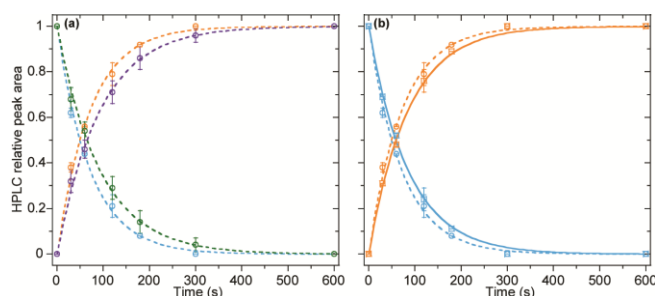
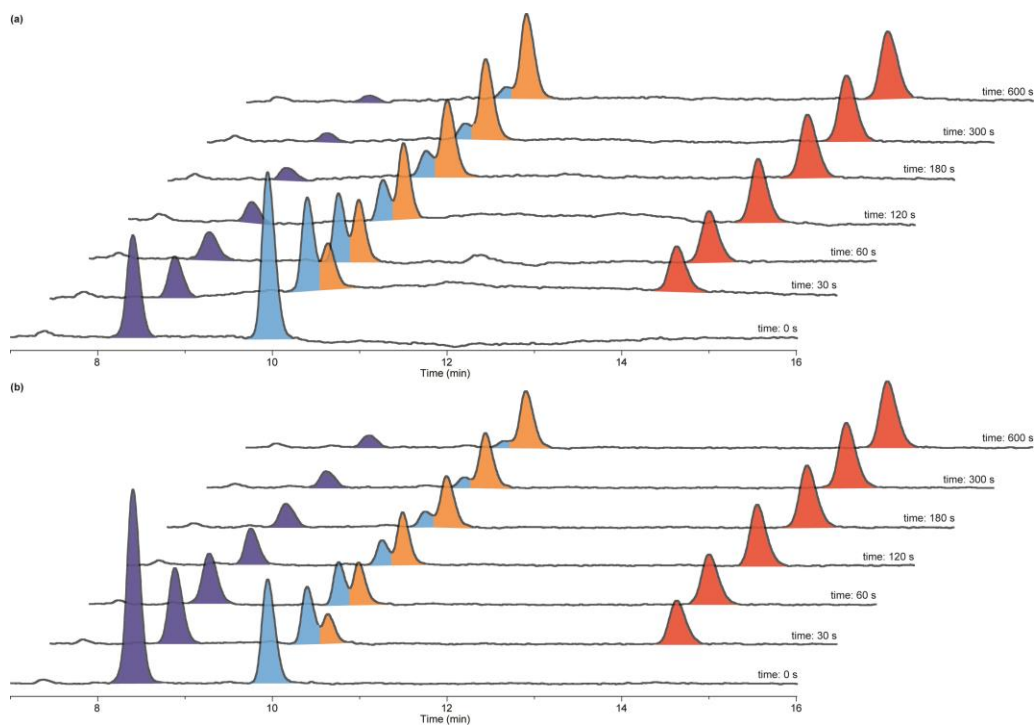
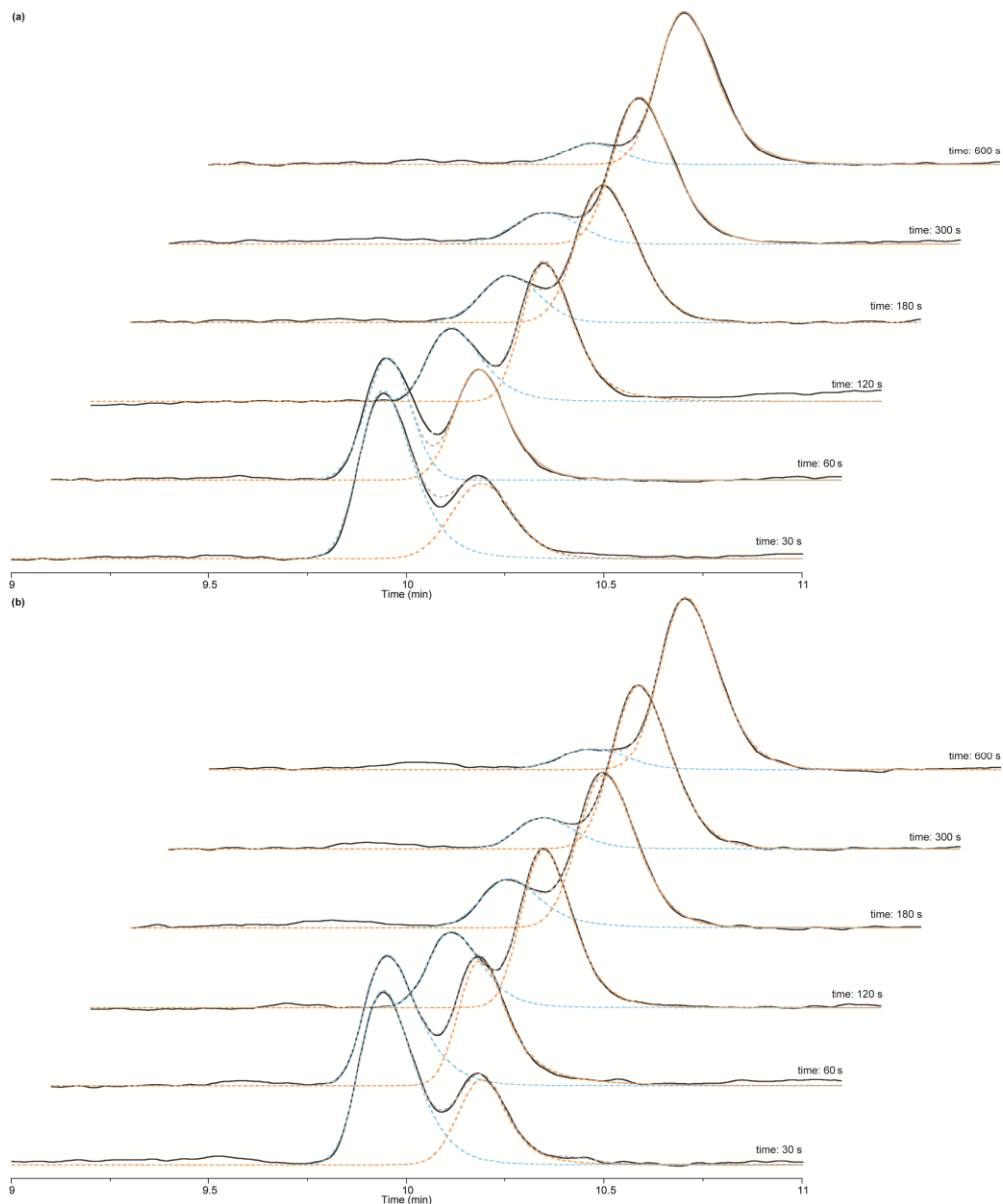


Figure S14. (a) Enzymatic competitive deamination of t^2 -AA (cyan) and native **A** (green) to provide t^2 G (orange) and **I** (purple) monitored by HPLC relative peak area variation at different time-points monitored at 260 nm. (b) HPLC relative peak area variation at different time points monitored at 260 (dashed) and 330 (solid) nm for the ADA competitive deamination of t^2 A (cyan) in presence of native **A** to generate t^2 G (orange) and **I**.



FigureS15. ADA-mediated competitive deamination analysis by HPLC monitored at 260 (a) and 330 (b) nm. Chromatogram showing the time course of enzymatic conversion of isomolar concentrations of t^2 -AA (cyan) and t^2 -A (blue) converted to t^2 -G (orange) and t^2 -I (red). Each set shows six time points following the addition of ADA.



FigureS16. HPLC peaks deconvolution at 260 (a) and 330 (b) nm. Chromatogram showing the time course of enzymatic competitive conversion of t^2 -AA (cyan) to t^2 G (orange) and t^2 A to t^2 I. Each time-set shows the observed chromatogram (black solid), the generated signal (grey dashed), the deconvoluted peak for t^2 -AA (cyan dashed) and t^2 G (dashed orange).

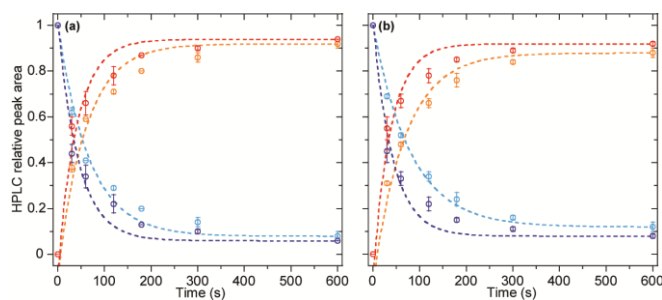
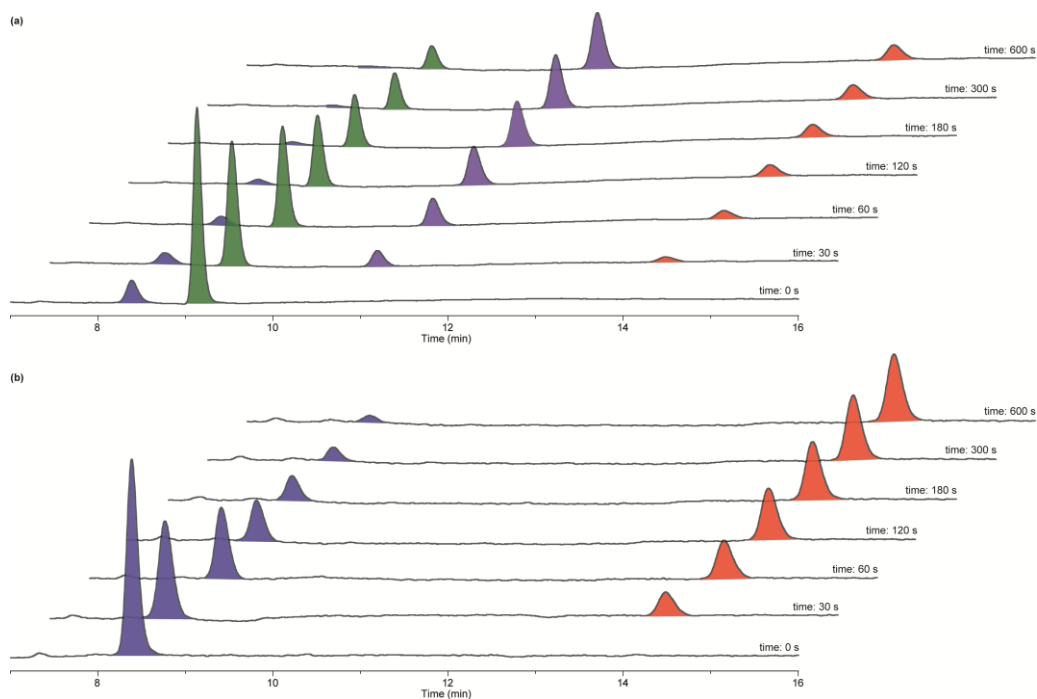


Figure S17. Enzymatic competitive deamination of t^2 -AA (cyan) and native t^2 A (blue) to provide t^2 G (orange) and t^2 I (red) monitored by HPLC relative peak area variation at different time-points monitored at 260 (a) and 330 (b) nm.



FigureS18. ADA-mediated competitive deamination analysis by HPLC monitored at 260 (a) and 330 (b) nm. Chromatogram showing the time course of enzymatic conversion of isomolar concentrations of ^{t2}A (blue) and A (green) converted to ^{t2}I (red) and I (purple). Each set shows six time points following the addition of ADA.

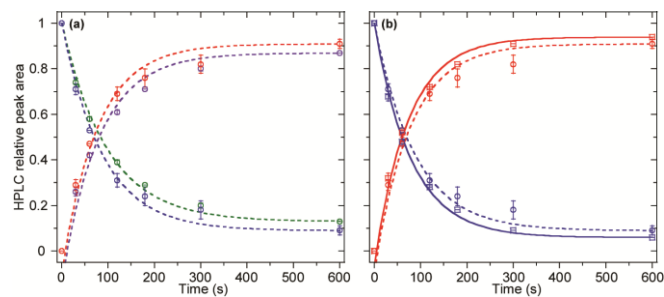


Figure S19. (a) Enzymatic competitive deamination of ^{t2}A (blue) and native A (green) to provide ^{t2}I (red) and I (purple) monitored by HPLC relative peak area variation at different time-points monitored at 260 nm. (b) HPLC relative peak area variation at different time points monitored at 260 (dashed) and 330 (solid) nm for the ADA competitive deamination of ^{t2}A (blue) in presence of native A to generate ^{t2}I (red) and I.

Table S8. Enzyme mediated adenosine deaminase initial rate – HPLC-based assay

| System | Species | λ_{montr}^a | k_1^b (10^{-3} s^{-1}) | $t_{1/2}^c$ (s) | Conversion ^d (%) |
|----------------------|---------------|----------------------------|---|--------------------|--------------------------------|
| tz2-AA/tzG | tz2-AA to tzG | 260 | 20.9±0.2 | 33.2±0.2 | 100 |
| | | 330 | 18.5±0.2 | 37.4±0.4 | |
| tz2-AA/tzG + A/I | tz2-AA to tzG | 260 | 13.0±0.4 | 53.2±0.3 | 100 |
| | | 330 | 11.8±0.3 | 58.8±0.4 | |
| tz2-AA/tzG + tzA/tzI | A to I | 260 | 10.8±0.09 | 64.3±0.4 | 100 |
| | tz2-AA to tzG | 260 | 14.0±0.3 | 50±1 | 88 |
| | | 330 | 12.4±0.4 | 56±3 | |
| | tzA to tzI | 260 | 23.3±0.5 | 29.7±0.9 | 92 |
| | | 330 | 23.9±0.2 | 29±1 | |
| tzA/tzI + A/I | tzA to tzI | 260 | 12.4±0.6 | 56±1 | 94 |
| | | 330 | 12.7±0.4 | 54.5±0.7 | |
| | A to I | 260 | 10.5±0.1 | 66±1 | 87 |

^a λ_{montr} is in nm and represent the followed wavelength in the specific experiment. ^b Pseudo first order reaction kinetic value determined by fitting the HPLC normalized area with non-linear regression function. ^c $t_{1/2}$ is the reaction half-time calculated assuming a pseudo first-order enzymatic kinetic and reflect the average over three independent measurements. ^d Conversion into the corresponding product after 600 second determined by HPLC peak area.

6. Supplementary figures

6.1. ^1H and ^{13}C NMR spectra

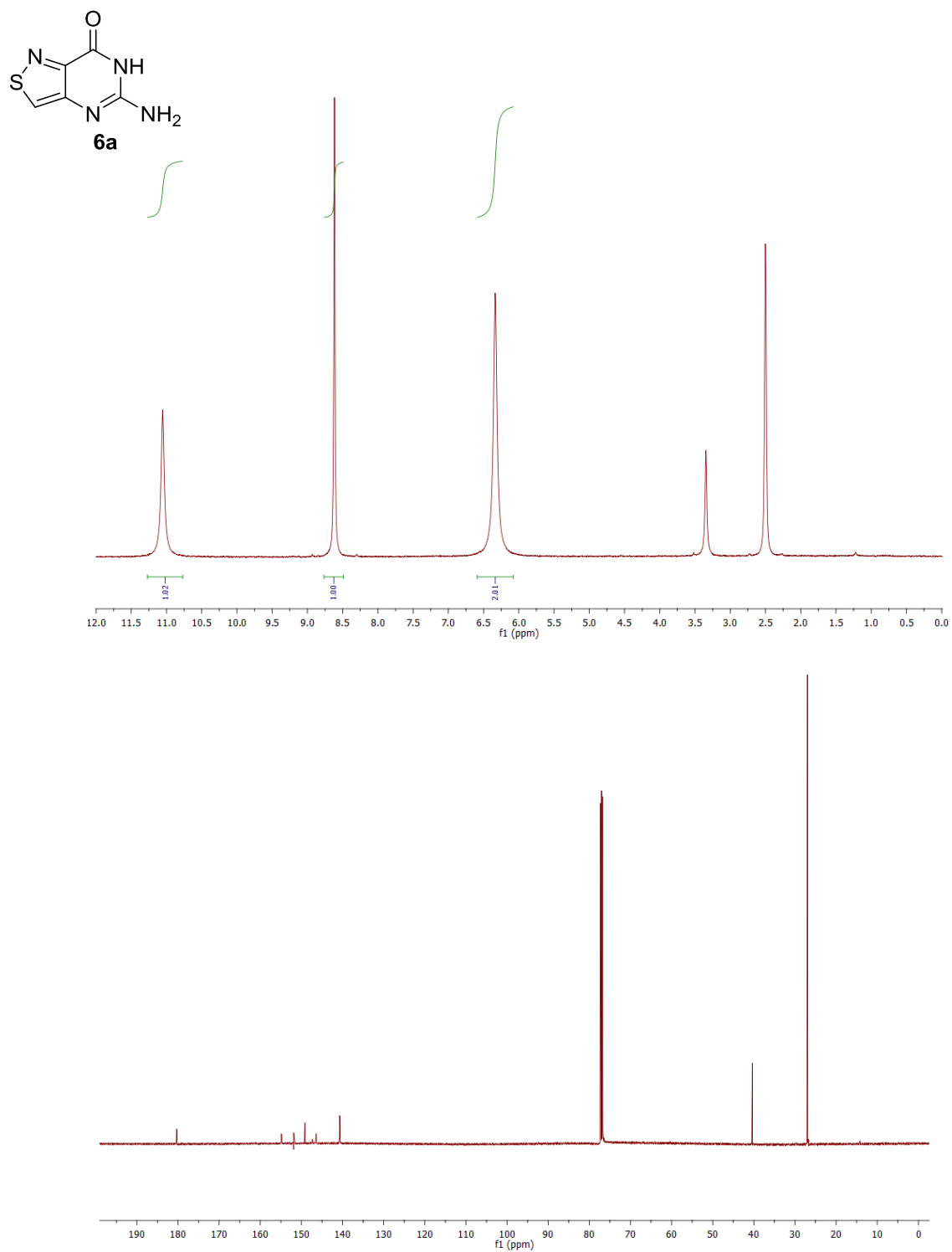


Figure S20. ^1H and ^{13}C NMR spectra of **6a**.

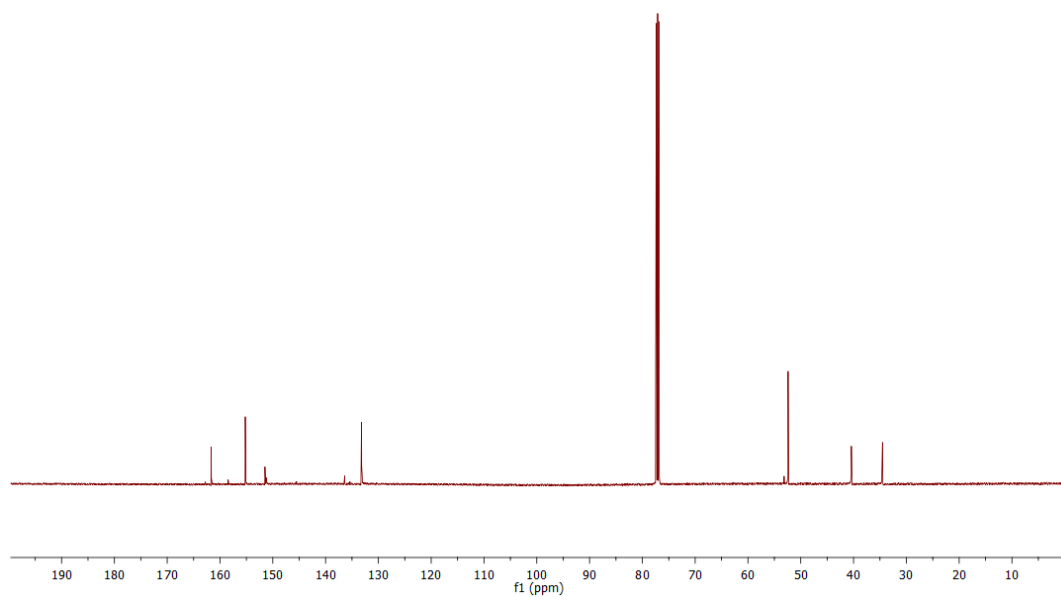
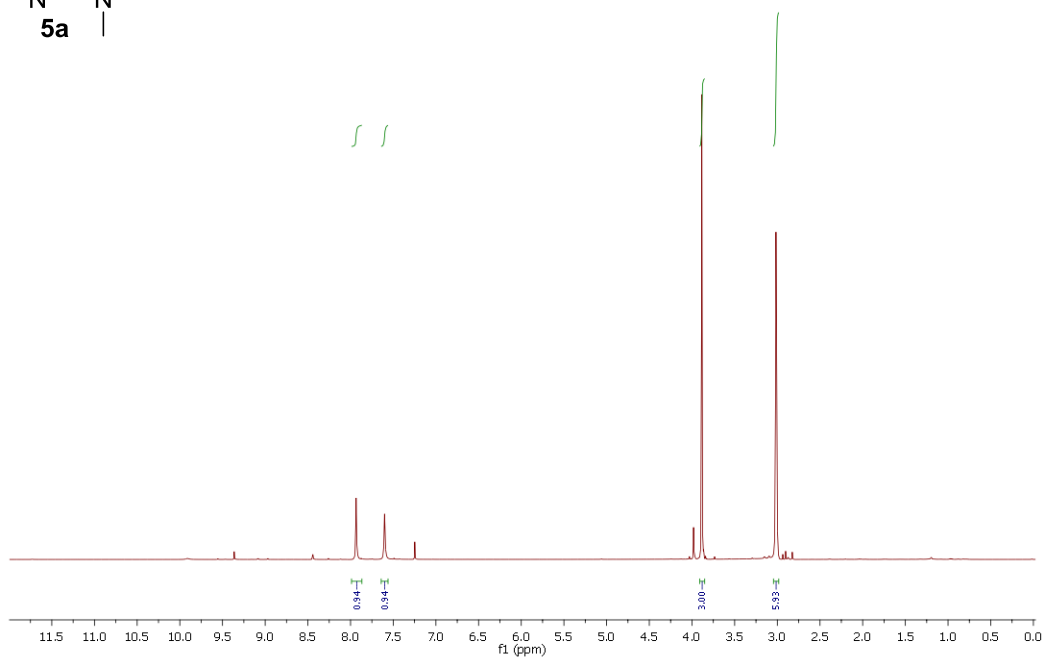
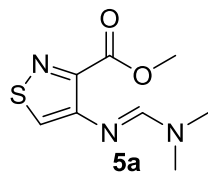


Figure S21. ¹H and ¹³C NMR spectra of **5a**.

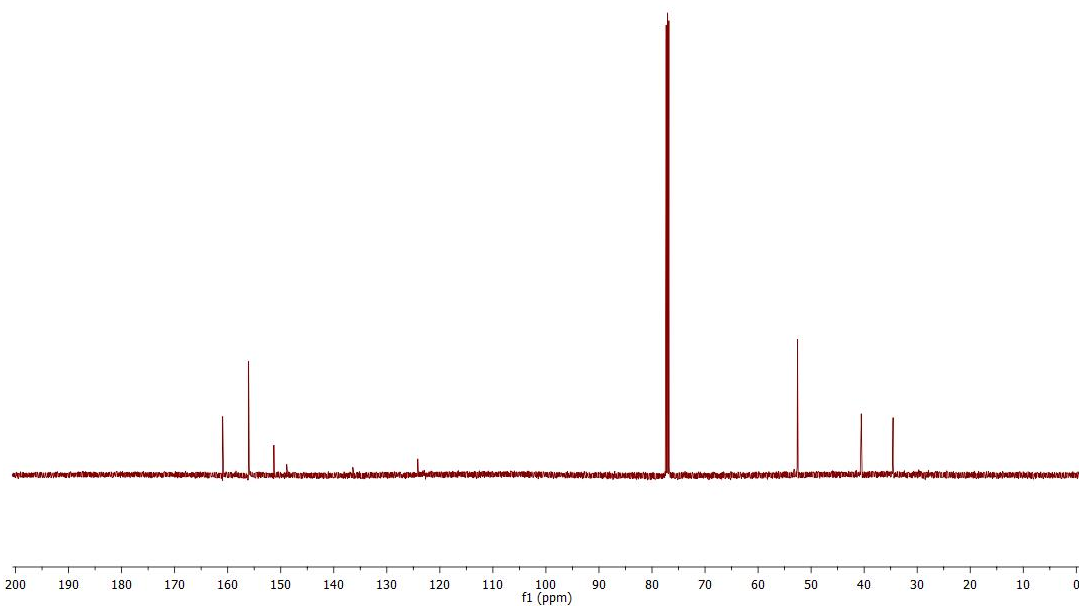
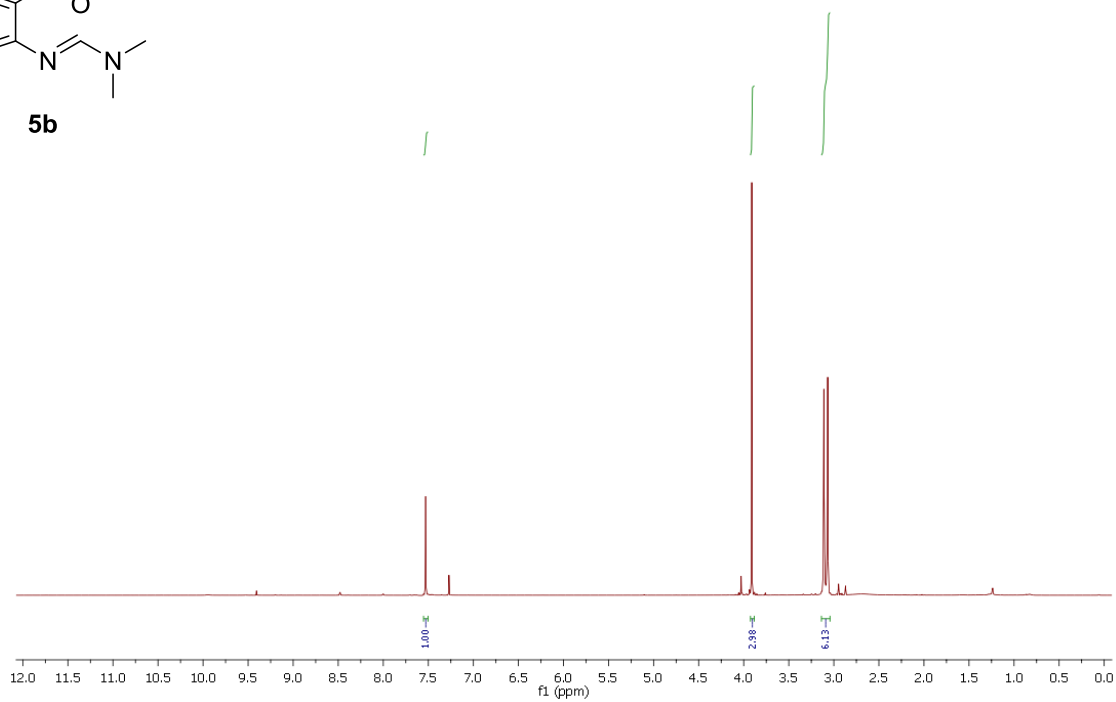
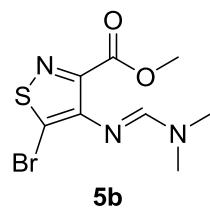


Figure S22. ^1H and ^{13}C NMR spectra of **5b**.

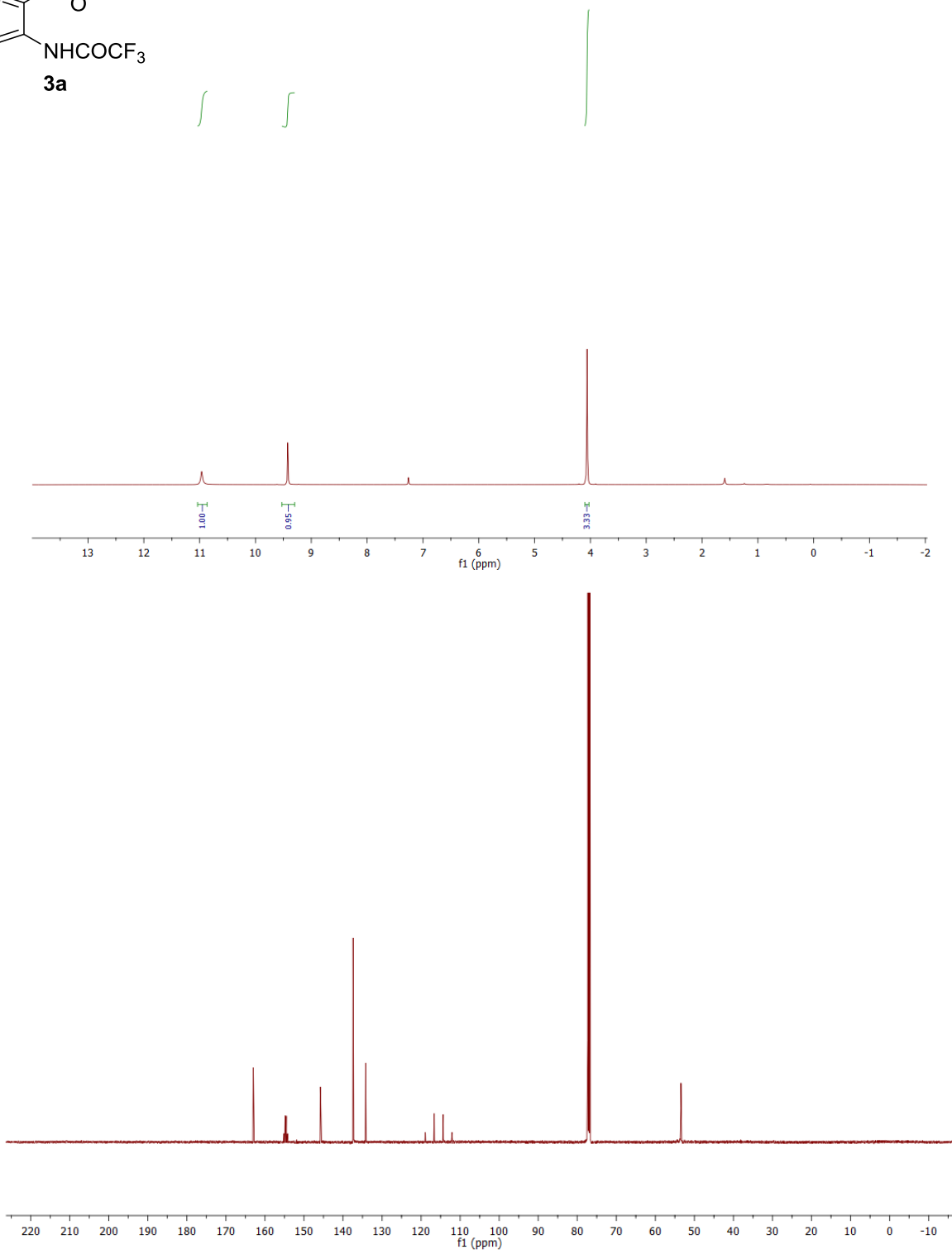
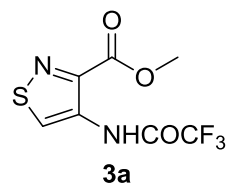


Figure S23. ¹H and ¹³C NMR spectra of 3a.

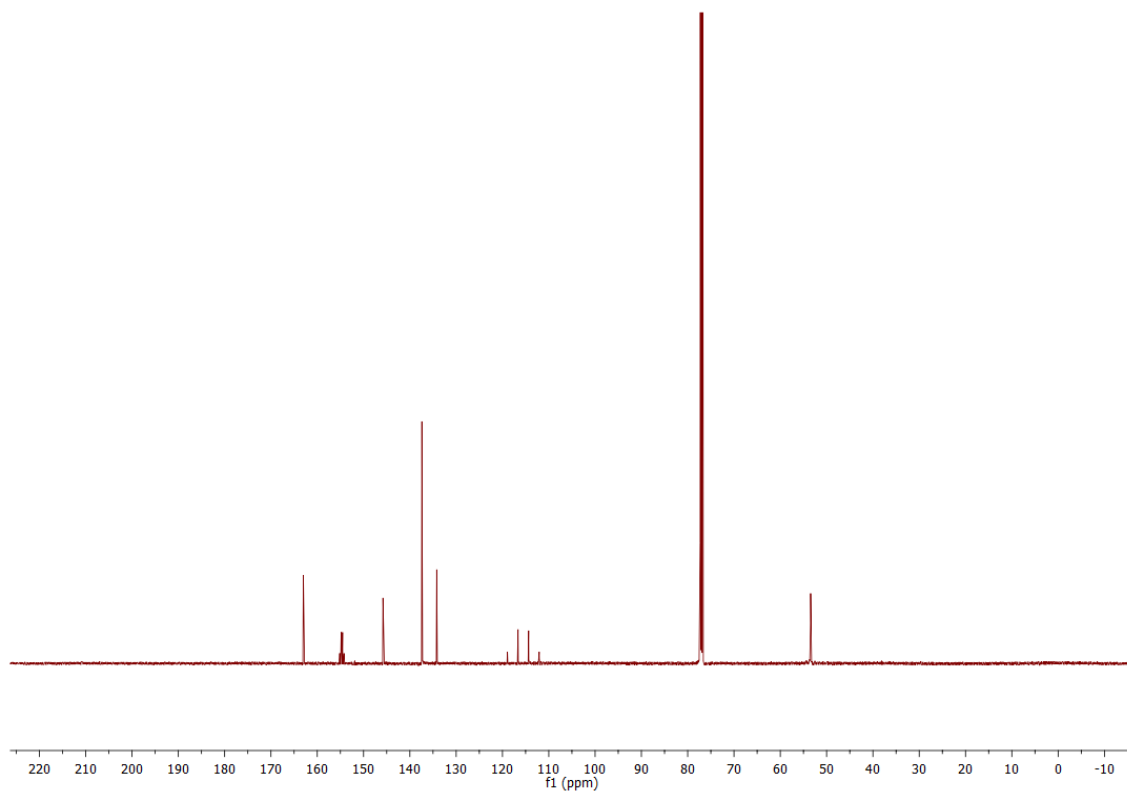
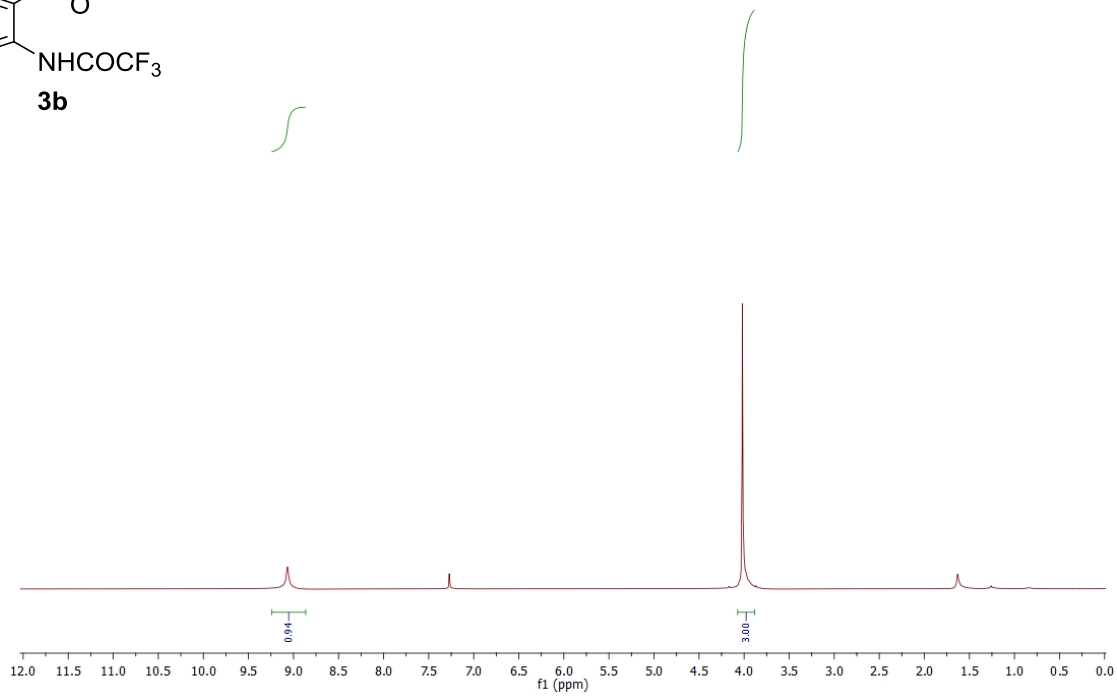
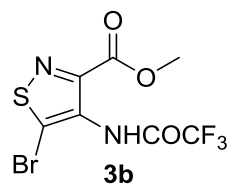


Figure S24. ^1H and ^{13}C NMR spectra of **3b**

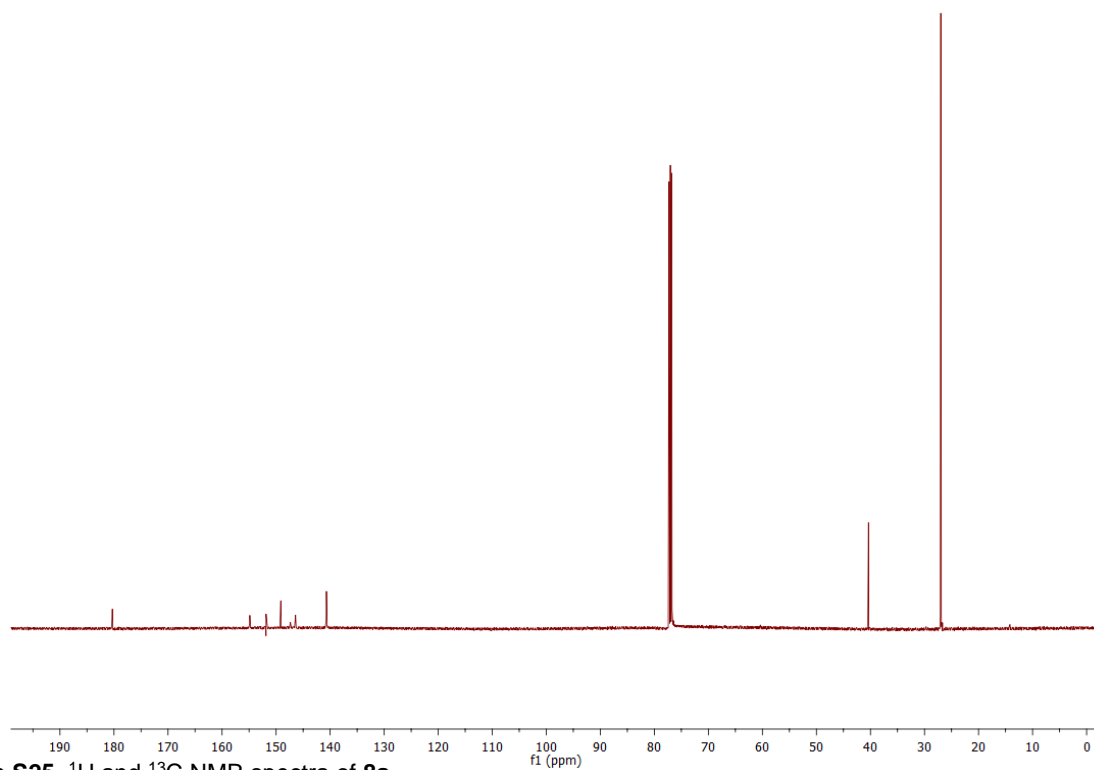
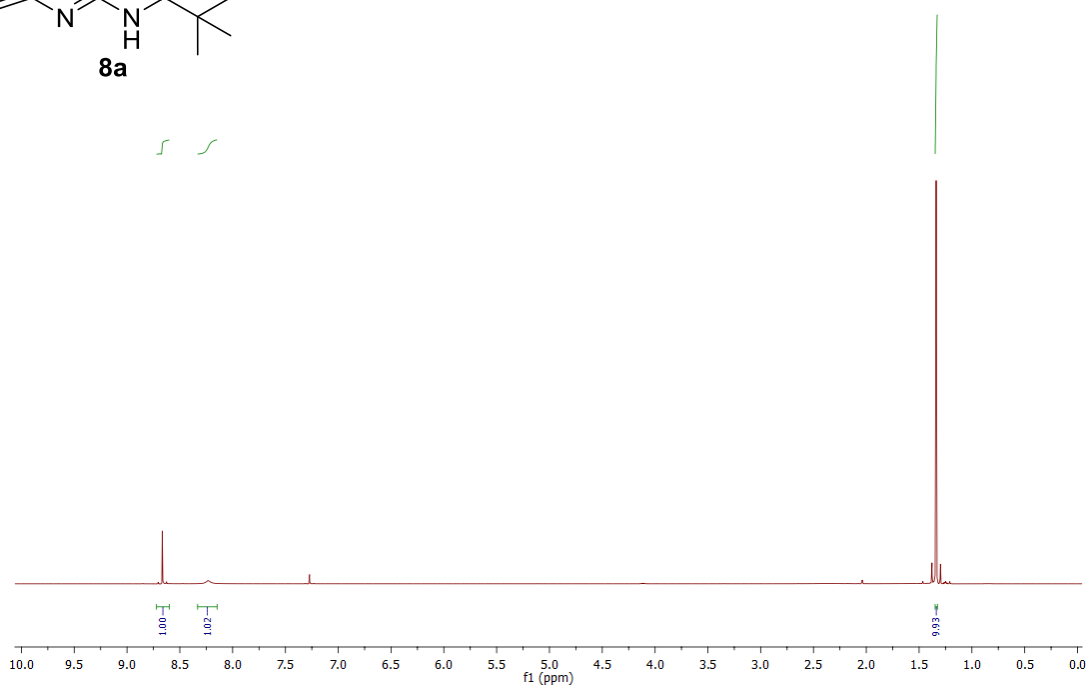
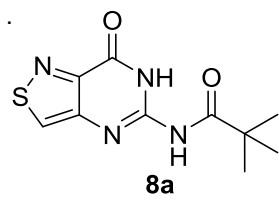


Figure S25. ¹H and ¹³C NMR spectra of **8a**

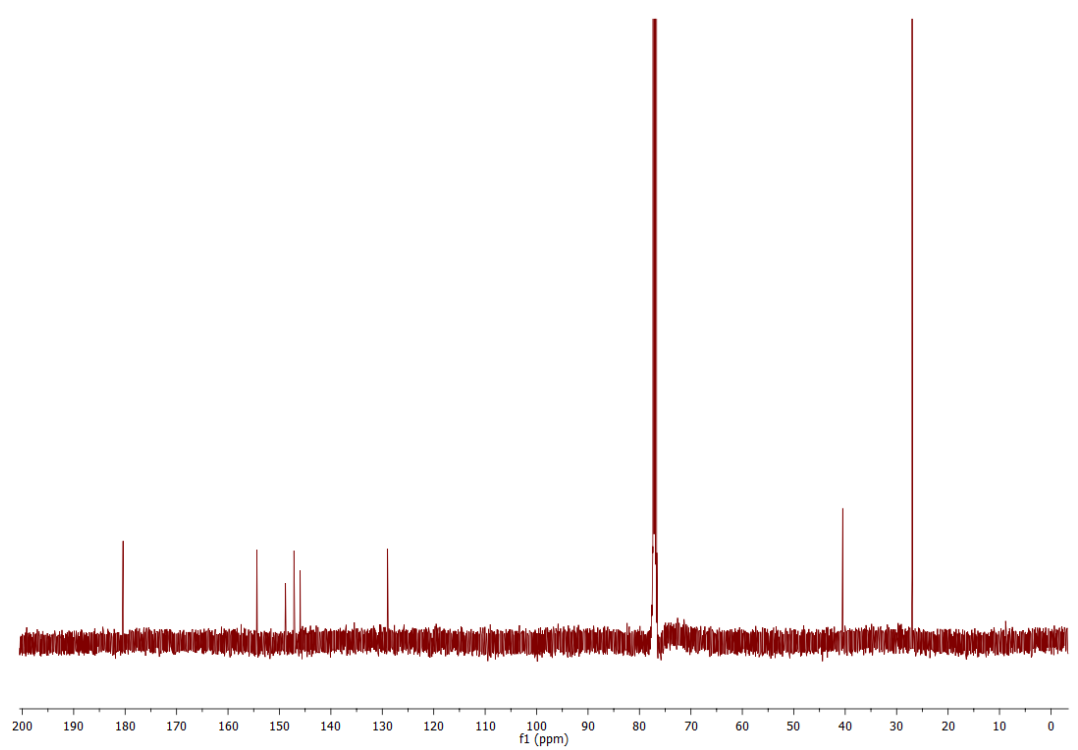
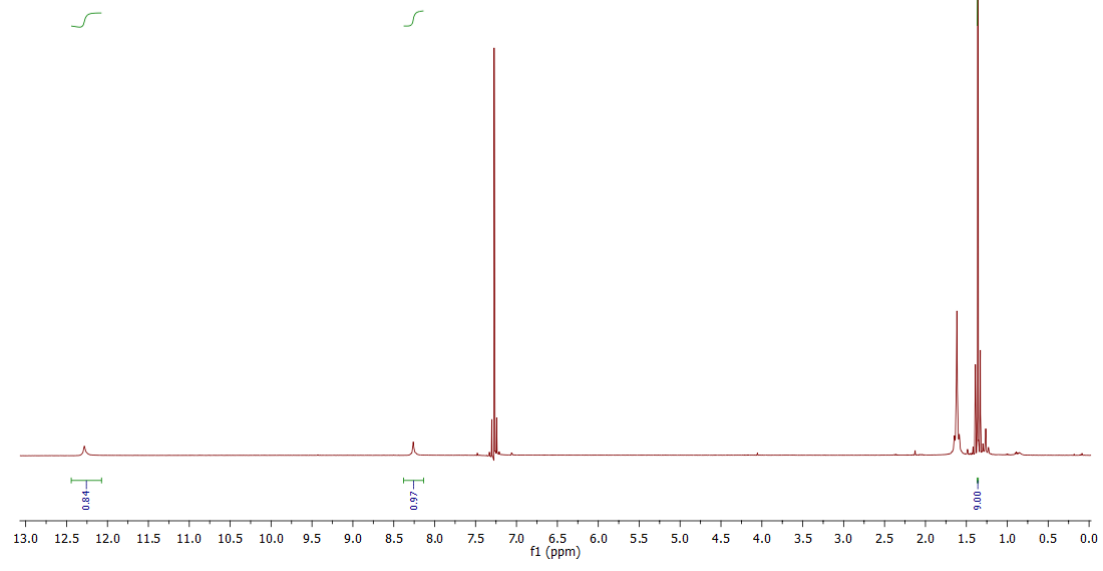
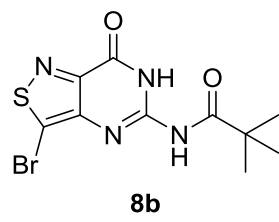


Figure S26. ¹H and ¹³C NMR spectra of **8b**

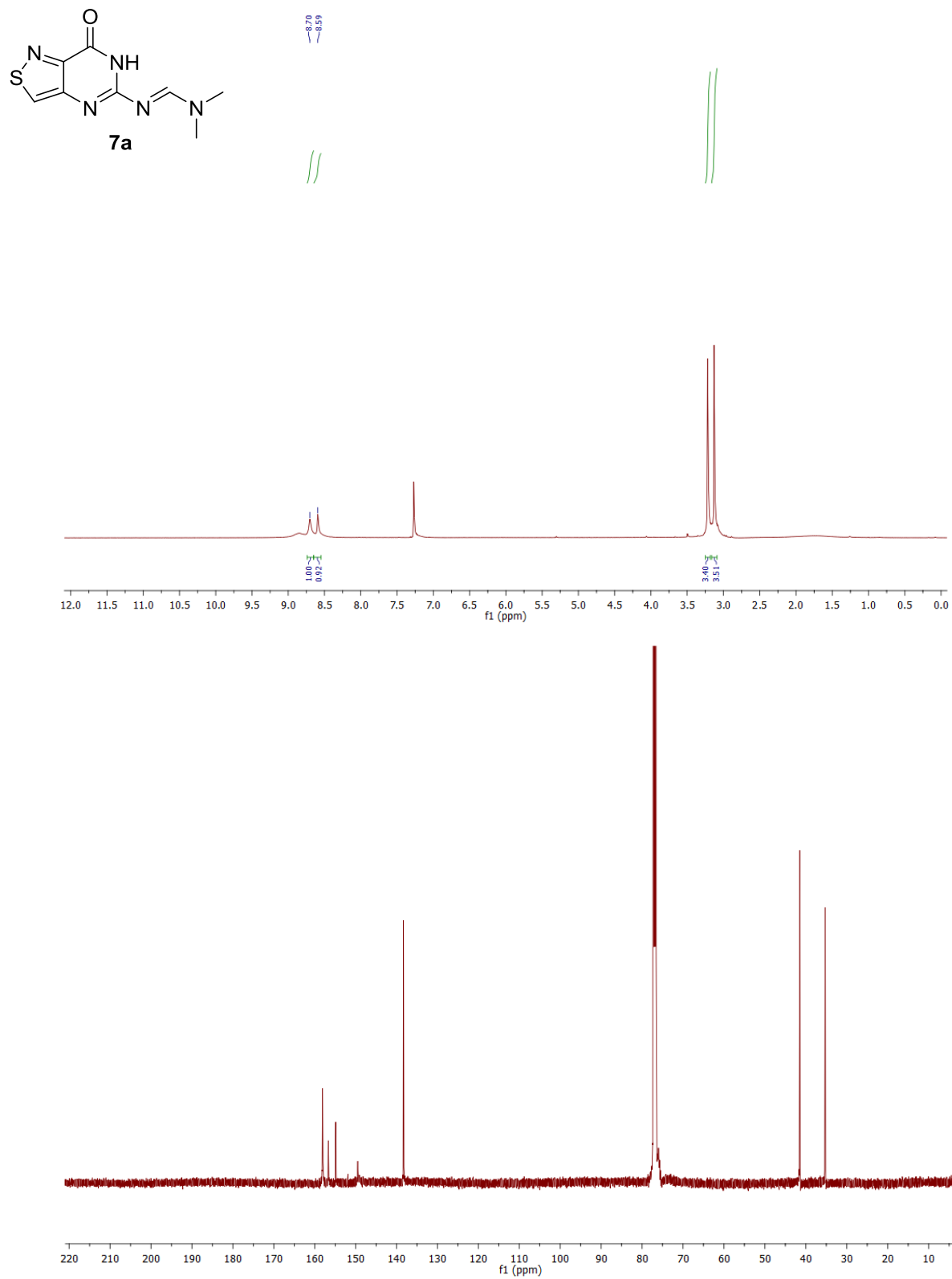


Figure S27. ^1H and ^{13}C NMR spectra of **7a**

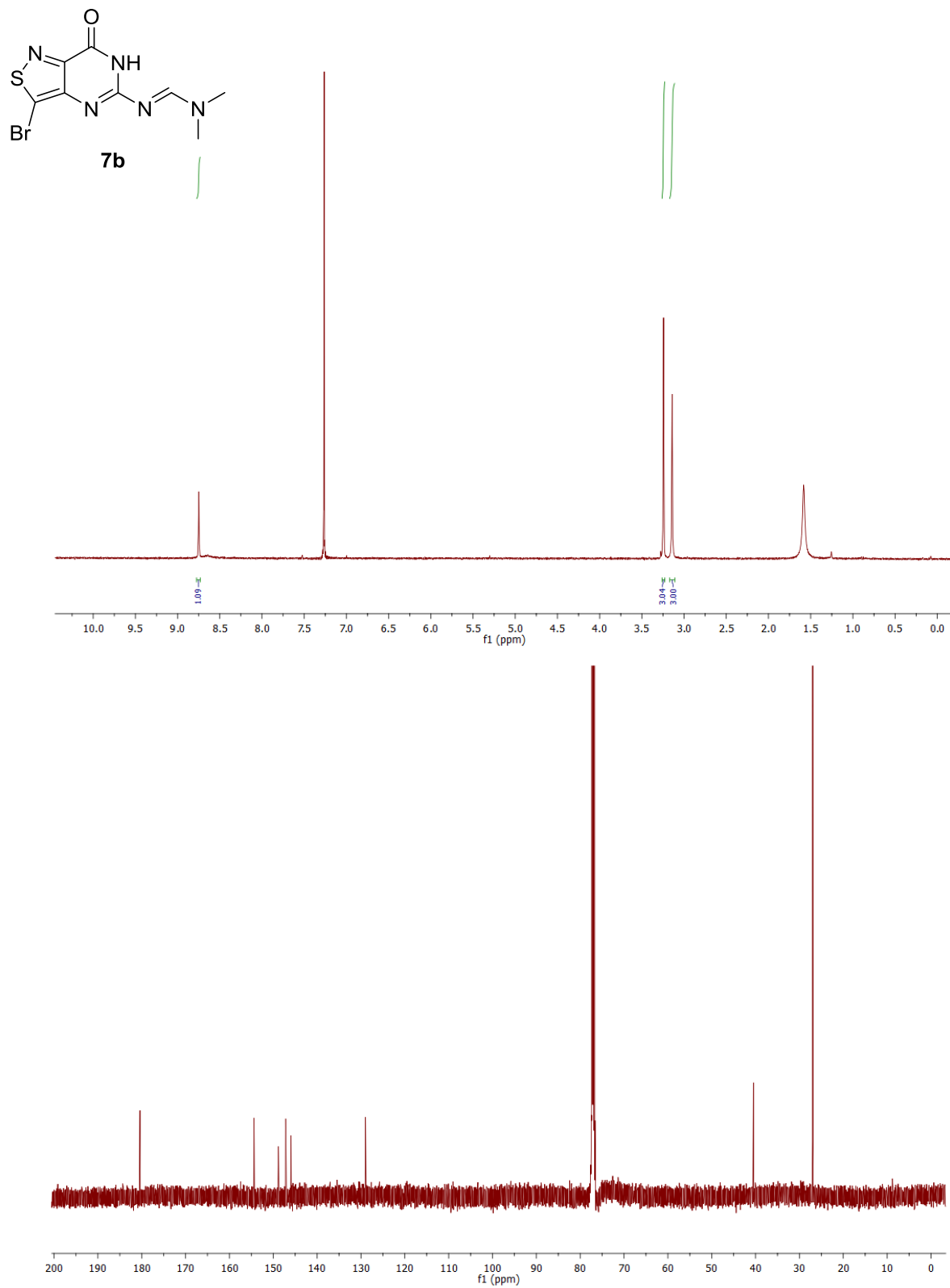


Figure S28. ¹H and ¹³C NMR spectra of **7b**

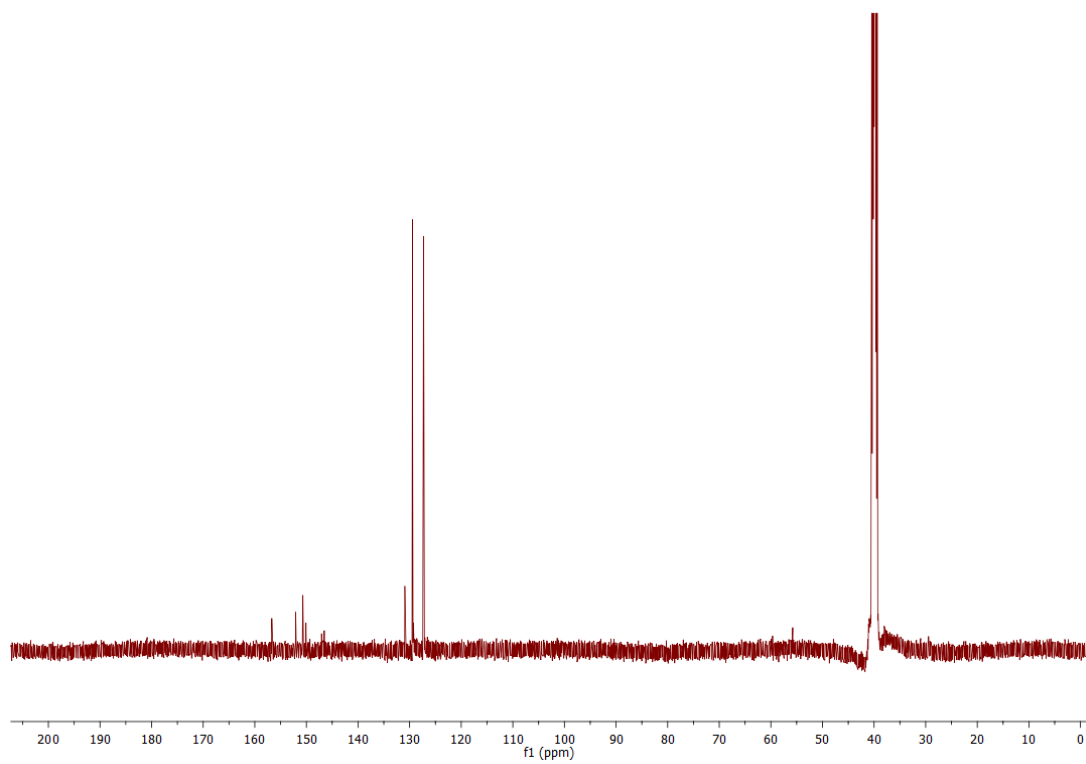
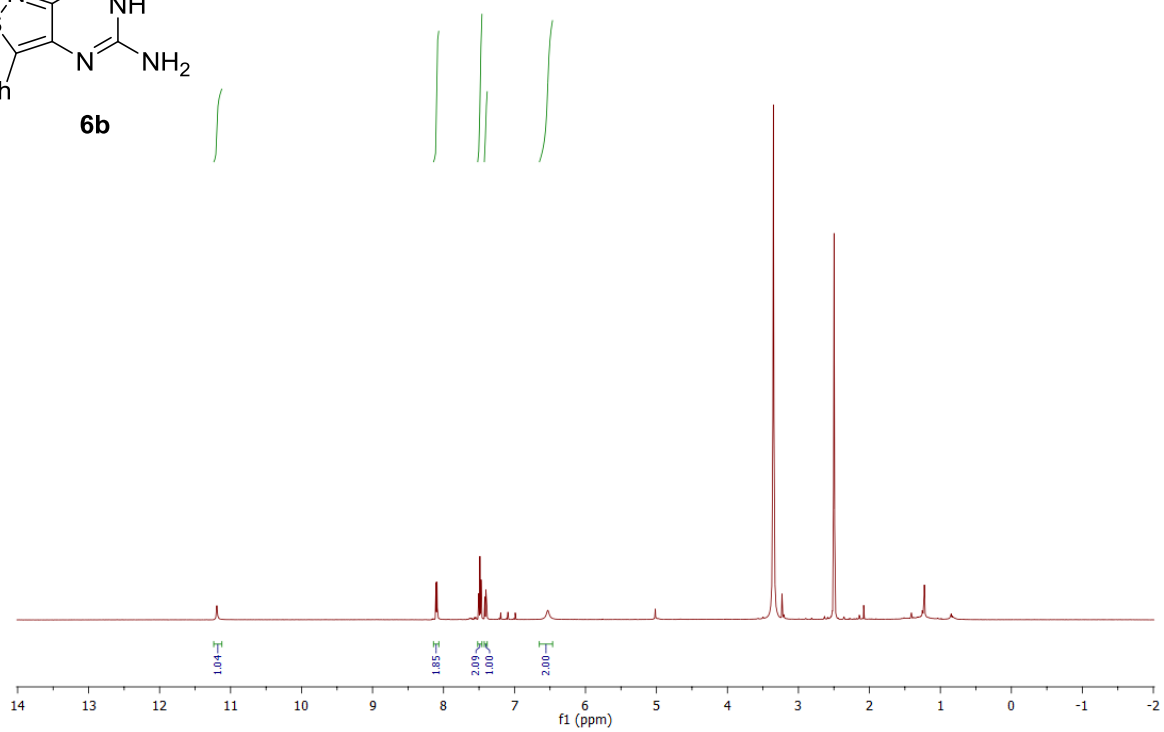
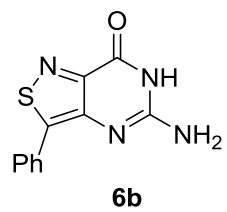


Figure S29. ¹H and ¹³C NMR spectra of **6b**

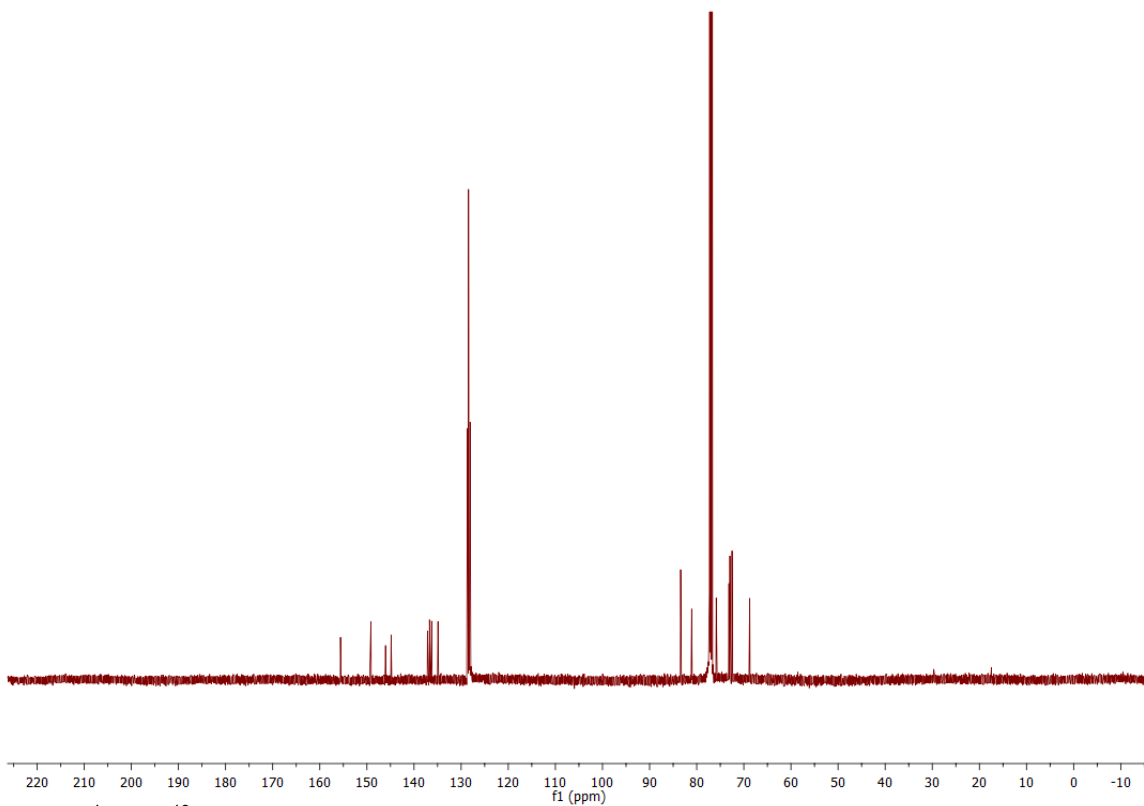
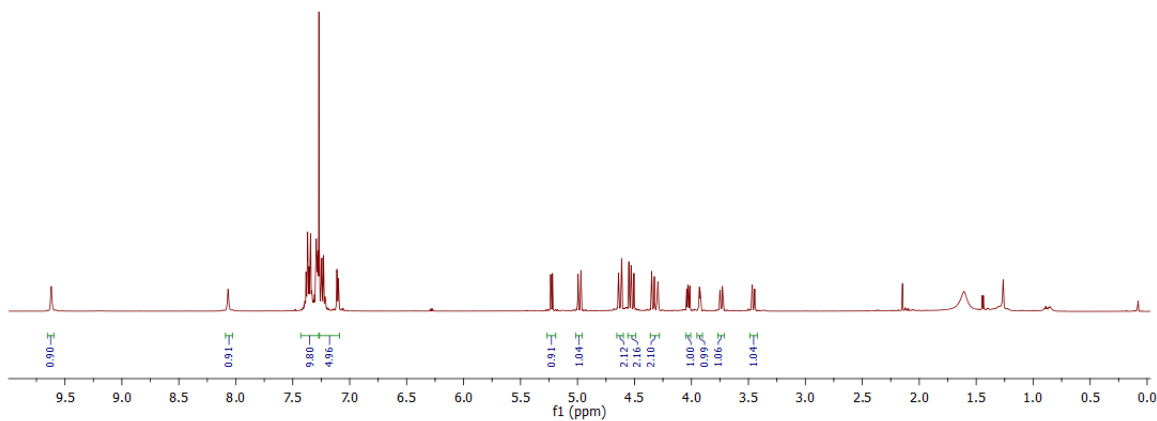
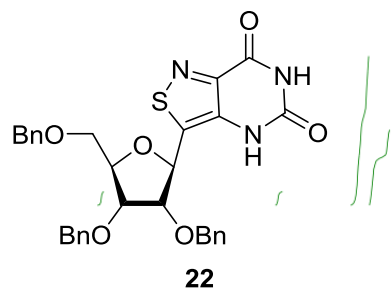


Figure S30. ^1H and ^{13}C NMR spectra of **22**

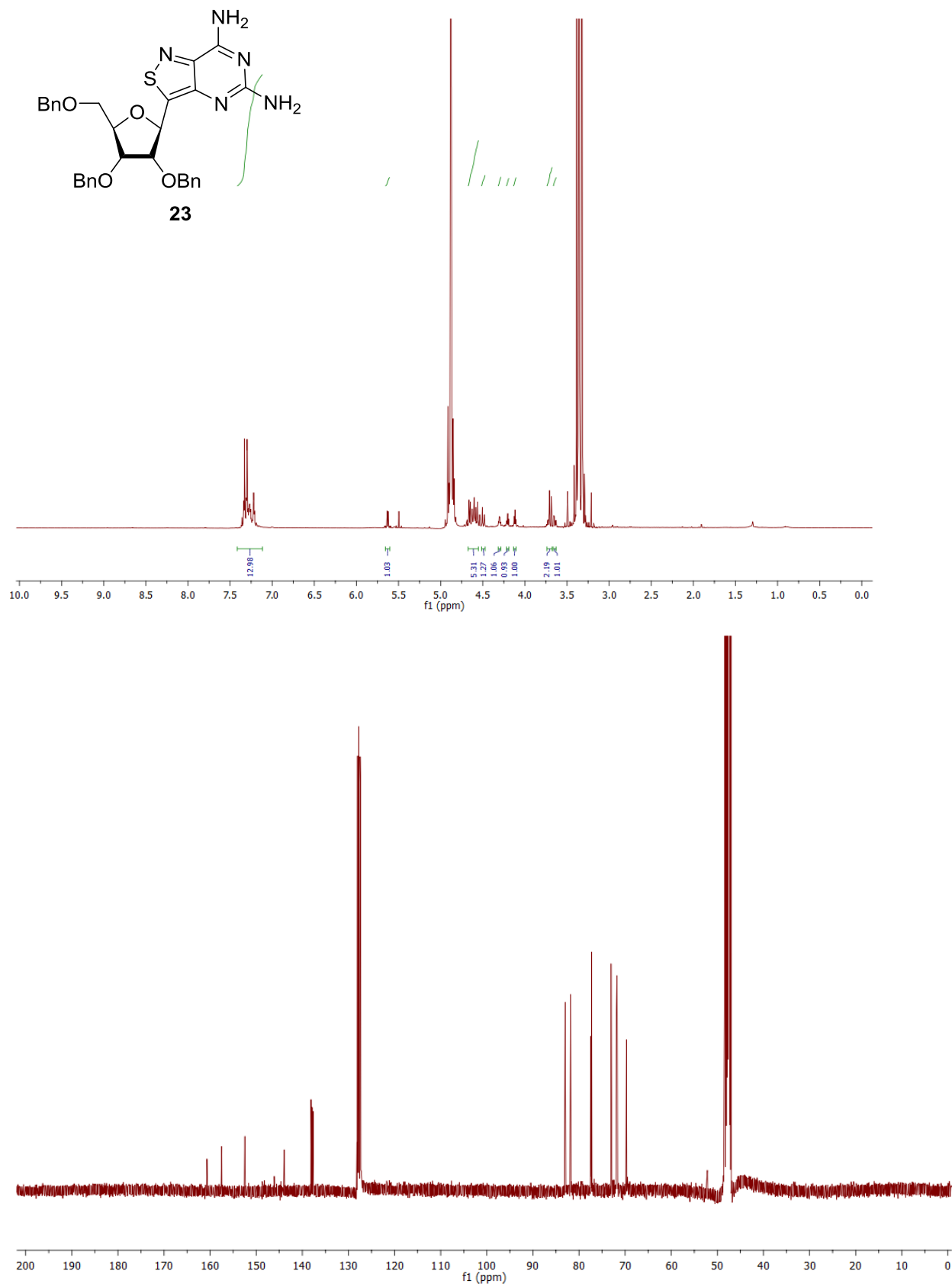


Figure S31. ¹H and ¹³C NMR spectra of **23**

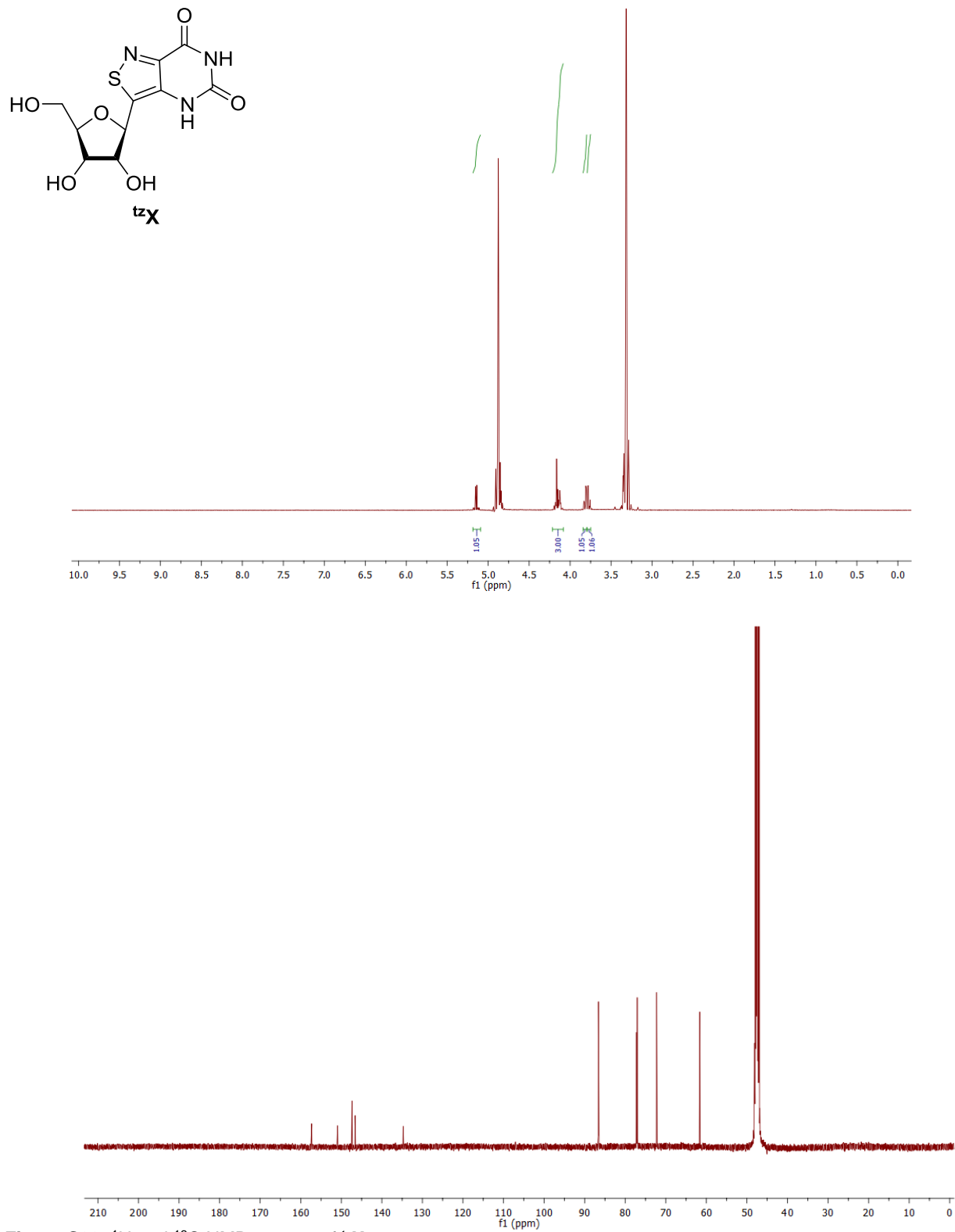


Figure S33. ¹H and ¹³C NMR spectra of **tzX**

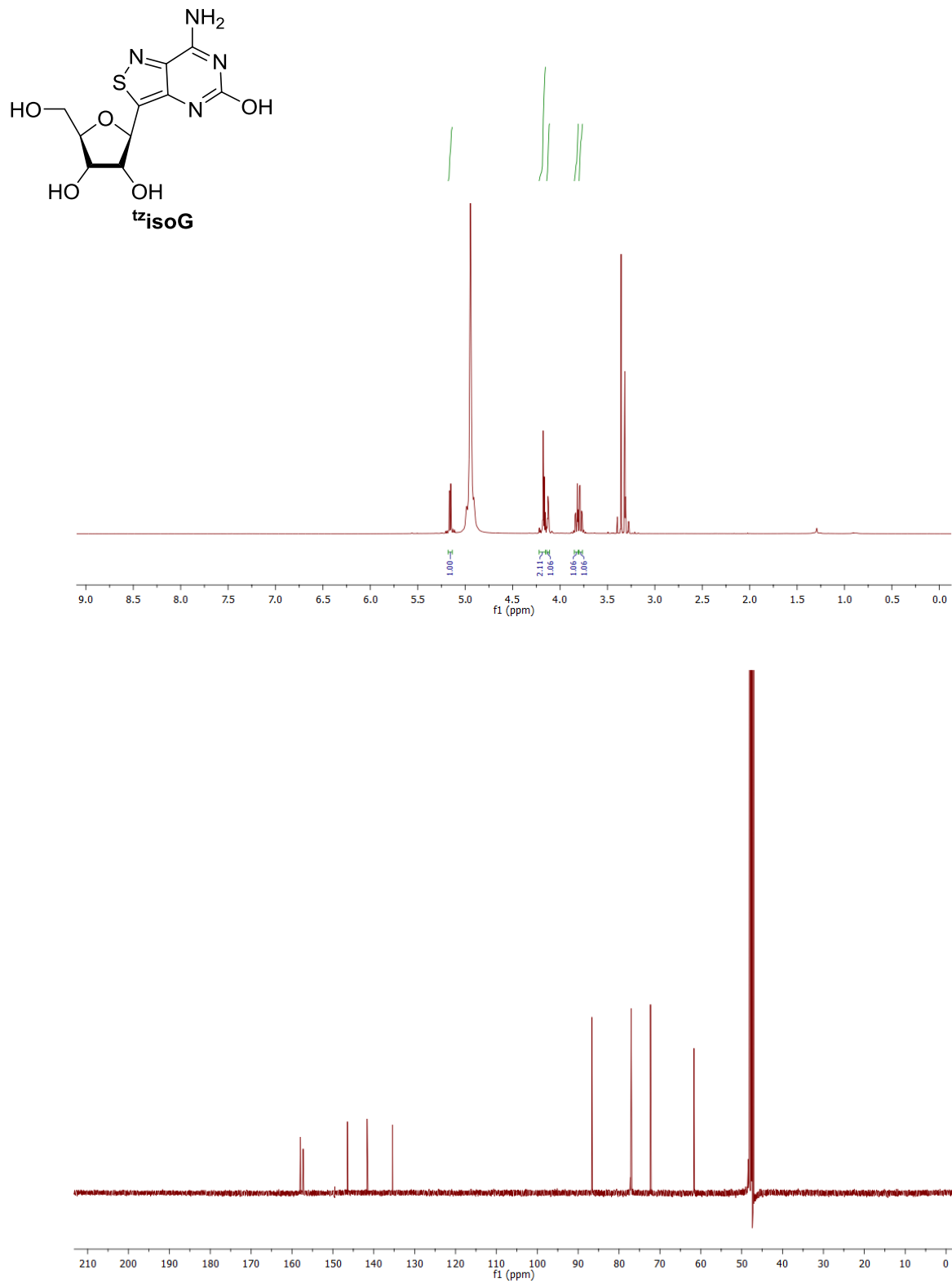


Figure S34. ^1H and ^{13}C NMR spectra of **tzIsoG**

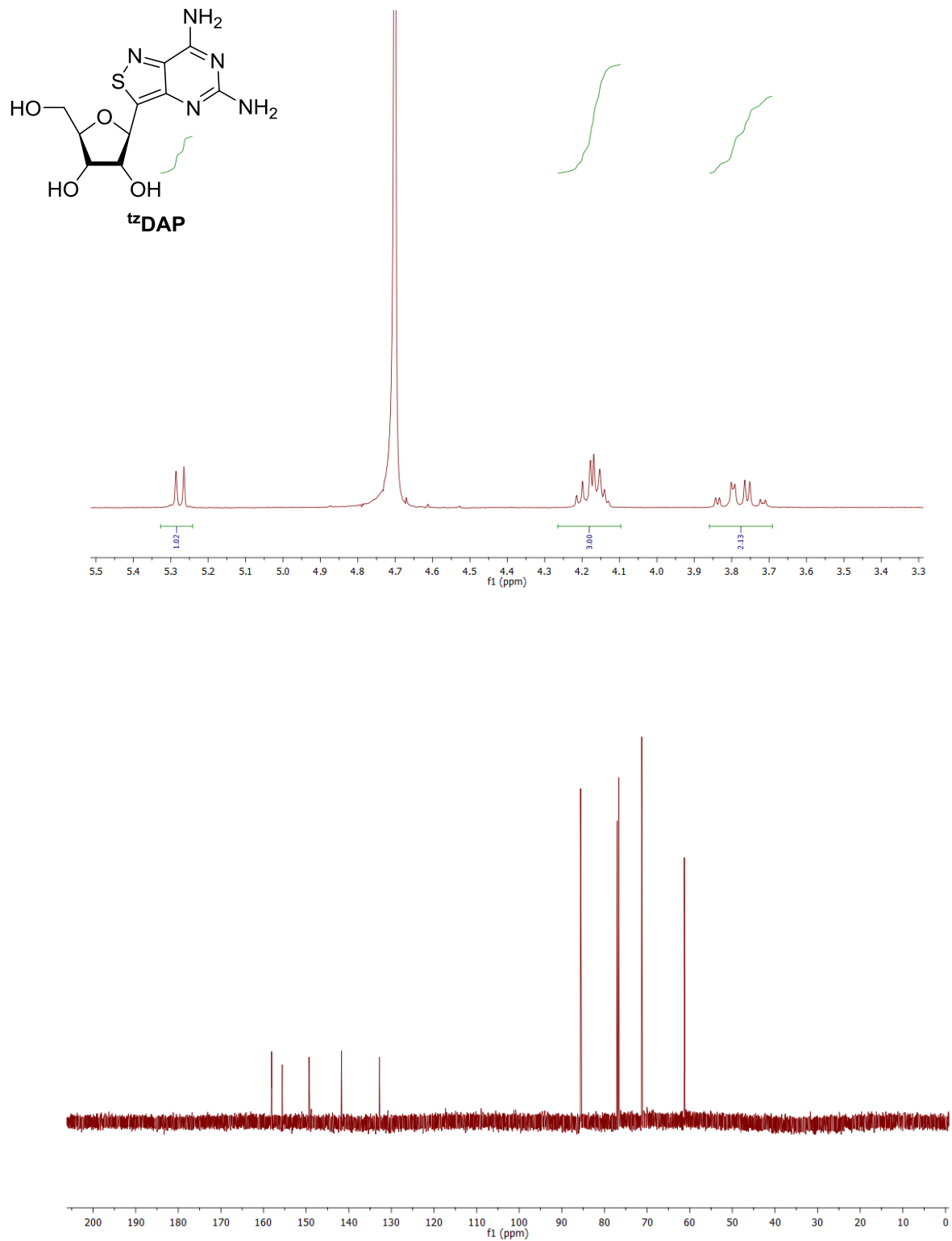


Figure S35. ^1H and ^{13}C NMR spectra of **tzDAP**

7. Supplementary references

- S1. A. R. Rovira, A. Fin and Y. Tor, *J. Am. Chem. Soc.*, 2015, **137**, 14602-14605.
- S2. E. A. Henderson, V. Bavetsias, D. S. Theti, S. C. Wilson, R. Clauss and A. L. Jackman, *Bioorgan Med Chem*, 2006, **14**, 5020-5042.
- S3. K. Temburnikar, Z. Zhang and K. Seley-Radtke, *Nucleos. Nucleot. Nucl.*, 2012, **31**, 319-327.
- S4. D. W. Shin and C. Switzer, *Chem. Commun.*, 2007, **42**, 4401-4403.
- S5. B. Lesyng, C. Marck and W. Saenger, *Z. Naturforsch C*, 1984, **39**, 720-724.
- S6. E. M. Kosower, H. Dodiuk and H. Kanety, *J. Am. Chem. Soc.*, 1978, **100**, 4179-4188.